WESTERDIJK FUNGAL BIO DIVERSITY INSTITUTE

Cyclins in aspergilli: Phylogenetic and functional analyses of group I cyclins

V. Paolillo[1], C.B. Jenkinson[1], T. Horio[2], and B.R. Oakley[1*]

[1]*Department of Molecular Biosciences, University of Kansas, 1200 Sunnyside Ave., Lawrence, KS 66045, USA;* [2]*Department of Natural Sciences, Nippon Sport Science University, Yokohama, Japan*

**Correspondence*: B. R. Oakley, boakley@ku.edu

Abstract: We have identified the cyclin domain-containing proteins encoded by the genomes of 17 species of *Aspergillus* as well as 15 members of other genera of filamentous ascomycetes. Phylogenetic analyses reveal that the cyclins fall into three groups, as in other eukaryotic phyla, and, more significantly, that they are remarkably conserved in these fungi. All 32 species examined, for example, have three group I cyclins, cyclins that are particularly important because they regulate the cell cycle, and these are highly conserved. Within the group I cyclins there are three distinct clades, and each fungus has a single member of each clade. These findings are in marked contrast to the yeasts *Saccharomyces cerevisiae, Schizosaccharomyces pombe*, and *Candida albicans*, which have more numerous group I cyclins. These results indicate that findings on cyclin function made with a model *Aspergillus* species, such as *A. nidulans*, are likely to apply to other Aspergilli and be informative for a broad range of filamentous ascomycetes. In this regard, we note that the functions of only one *Aspergillus* group I cyclin have been analysed (NimE$^{Cyclin\ B}$ of *A. nidulans*). We have consequently carried out an analysis of the members of the other two clades using *A. nidulans* as our model. We have found that one of these cyclins, PucA, is essential, but deletion of PucA in a strain carrying a deletion of CdhA, an activator of the anaphase promoting complex/cyclosome (APC/C), is not lethal. These data, coupled with data from heterokaryon rescue experiments, indicate that PucA is an essential G_1/S cyclin that is required for the inactivation of the APC/C-CdhA, which, in turn, allows the initiation of the S phase of the cell cycle. Our data also reveal that PucA has additional, non-essential, roles in the cell cycle in interphase. The *A. nidulans* member of the third clade (AN2137) has not previously been named or analyzed. We designate this gene *clbA*. ClbA localizes to kinetochores from mid G_2 until just prior to chromosomal condensation. Deletion of *clbA* does not affect viability. However, by using a regulatable promoter system new to *Aspergillus*, we have found that expression of a version of ClbA in which the destruction box sequences have been removed is lethal and causes a mitotic arrest and a high frequency of non-disjunction. Thus, although ClbA is not essential, its timely destruction is essential for viability, chromosomal disjunction, and successful completion of mitosis.

Key words: Aspergilli, Cyclins, Cell cycle, Phylogeny.

Available online 20 June 2018; https://doi.org/10.1016/j.simyco.2018.06.002.

INTRODUCTION

The eukaryotic cell cycle is driven by the periodic synthesis and destruction of cyclins that bind and activate a class of serine/threonine kinases called cyclin-dependent kinases (CDKs). Distinct cyclin/CDK complexes form and become active at different stages of the cell cycle. Once a cyclin has completed its function, it is targeted for destruction, inactivating its partner CDK. The formation of cyclin/CDK complexes and subsequent cyclin destruction drives the cell through G_1, S, G_2 and mitosis in a sequential and irreversible manner. In addition to cell cycle regulation, cyclin/CDK complexes function in a variety of cellular processes, such as transcriptional regulation, the ubiquitin-proteasome pathway, epigenetic events, metabolism, stem cell self-renewal, neuronal function, spermatogenesis, and the DNA damage response [reviewed in Lim & Kaldis (2013)]. Interestingly, there is also evidence that some of these non-canonical functions are carried out by cyclins independent of kinase activity [reviewed in Hydbring *et al.* (2016)].

Recent phylogenetic analyses have revealed that cyclins from a variety of different eukaryotes, including yeasts, plants, and humans, can be divided into three major groups (Ma *et al.* 2013, Cao *et al.* 2014). Group I is composed of the "classic" cell cycle regulatory cyclins, while group III cyclins tend to function primarily in transcriptional regulation. Group II cyclins have varied functions that include, but are not limited to, roles in cell cycle regulation (Davidson *et al.* 2009, Jimenez *et al.* 2013) and development (Wu *et al.* 2004, Liu & Finley 2010, Mikolcevic *et al.* 2012, Zi *et al.* 2015). However, it is important to note that (1) these phylogenetic analyses incorporated cyclins from a small number of eukaryotes, (2) our understanding of cyclin function is derived from only a handful of model species, and (3) there has been relatively little study of cyclins in filamentous fungi.

Filamentous fungi are, of course, of huge ecological importance and have an enormous impact on human and animal health, agricultural crop production, and industrial production of important commodities (May & Adams 1997, Bok *et al.* 2006, Pagano *et al.* 2006, Nalley *et al.* 2016). An excellent recent commentary addressed our limited understanding of filamentous fungal biology, the threat filamentous fungi pose to the food supply and to human and animal health, and the critical need to advance fungal biotechnology (Meyer *et al.* 2016). There is, thus, every reason to investigate cyclin function and cell cycle regulation in filamentous fungi, to help us facilitate their growth when appropriate and inhibit their growth when needed. In addition, it will be of benefit to carry out phylogenetic and functional analyses of cyclins from additional organisms to further our understanding of eukaryotic cell cycle regulation and how these control systems evolved.

The budding yeast *Saccharomyces cerevisiae* and the fission yeast *Schizosaccharomyces pombe* are popular models for

Peer review under responsibility of Westerdijk Fungal Biodiversity Institute.

Studies in Mycology

studying the cell cycle, and cyclins have been studied extensively in these organisms. While one might imagine that these yeasts can be used as a "reference system" for filamentous fungi, and they are often cited as such in the literature, this is not the case [reviewed in Meyer *et al.* (2016)].

In this work we have investigated the cyclin repertoires in the filamentous fungi analysed in a recent comparative genomics study (de Vries *et al.* 2017). This group contains 17 species of the genus *Aspergillus* and 15 species from other, phylogenetically diverse, genera. [Note, *Aspergillus zonatus* which was included in the de Vries *et al.* (2017) study does not belong in the genus *Aspergillus* and has been reclassified as *Penicilliopsis zonata* (Kocsube *et al.* 2016)]. The list includes 23 species from the order Eurotiales (including *Aspergillus nidulans*), seven species from Onygenales, *Trichoderma reesi* from Hypocreales, and *Neurospora crassa* from Sordariales. The group is well chosen because it allows one to determine if there are commonalities within the aspergilli and if these commonalities are shared with other, diverse, filamentous ascomycetes. All species in this group fall within the subdivision Pezizomycotina that includes most ascomycetes. This group does not contain members of the Saccharomycotina which includes yeasts such as *S. cerevisiae*, dimorphic fungi such as *Candida albicans* and filamentous fungi such as *Ashbya gossypii* that are closely related to, and probably derived from yeasts, nor does our study group contain any member of the Taphrinomycotina such as *S. pombe* (Wang *et al.* 2009). Although basidiomycetes and oomycetes are of great interest, they are also outside of this study. Finally, to avoid repeated use of awkwardly long phrases, we will use the term "filamentous ascomycetes" to refer to members of the Pezizomycotina, which are by far the most numerous filamentous ascomycetes, realizing that there are some ascomycetes from outside of this subdivision that have a filamentous growth form.

Our phylogenetic analyses of cyclins in these 32 species of filamentous ascomycetes reveal that, as in other organisms that have been studied (Ma *et al.* 2013, Cao *et al.* 2014), cyclins fall into three groups. Strikingly, the complement of cyclins is remarkably conserved. For example, each species surveyed has three group I cyclins. These are particularly important because they typically play critical roles in the regulation of the cell cycle. The group I cyclins fall into three clades with each fungus having a single member of each clade. It follows that the cyclins in these phylogenetically diverse filamentous ascomycetes are likely to be functionally conserved. Lessons learnt from studying cyclin function in the model organism *A. nidulans*, are likely to apply across the genus *Aspergillus* and are likely to be informative with respect to many other filamentous ascomycetes, including pathogenic and industrially important species. Our analysis also reveals that the complement of cyclins found in these fungi is significantly different from that of yeast models. For example, *S. cerevisiae* has nine group I cyclins while *S. pombe* and *C. albicans* each have five. The yeasts are, thus, likely to be of limited value in understanding cyclin function in filamentous fungi.

Our analyses also highlight how under-studied the cyclins of aspergilli and other Pezizomycotina are. Only a single group I cyclin has been analysed thoroughly, NimE$^{\text{Cyclin B}}$ of *A. nidulans.* NimE$^{\text{Cyclin B}}$ (O'Connell *et al.* 1992) is a binding partner of the Cdk1 homolog NimX (Osmani *et al.* 1994). NimE$^{\text{Cyclin B}}$ is required for both S-phase and G_2/M and its destruction during mitosis is required for mitotic exit (De Souza *et al.* 2009, Nayak *et al.* 2010). Up to now, NimE$^{\text{Cyclin B}}$ is the only cyclin that has been shown to be essential in *A. nidulans* and the only cyclin shown to have clear, cell cycle-related functions. The other two *A. nidulans* group I cyclins are a named but uncharacterized cyclin, PucA, and a previously unstudied cyclin encoded by gene AN2137 [using the AspGD (http://aspgd.org/) and FungiDB (http://fungidb.org/fungidb/) gene designation].

Given the importance of group I cyclins and the dearth of data on the functions of these proteins in filamentous ascomycetes in general and aspergilli in particular, we have carried out a functional analysis of PucA and AN2137. Our genetic and live imaging data reveal that PucA is an essential G_1/S cyclin that is required for the inactivation of the anaphase promoting complex/cyclosome (APC/C) complexed with its binding partner CdhA. Deletion of the *pucA* gene is lethal, but viability is restored if the *cdhA* gene is also deleted. We designate AN2137, the previously unnamed B-type cyclin gene, *clbA*. ClbA localizes to kinetochores from mid-G_2 until just before chromosomal condensation. Deletion of *clbA* does not affect viability. Timely destruction of cyclins is critical for their function, and cyclins are normally targeted for destruction by APC/C binding to one or both of two conserved sequences called destruction boxes (d-boxes) or KEN boxes. Using a regulatable promoter system new to *A. nidulans*, we have found that expression of a version of ClbA in which the d-boxes have been removed results in a mitotic block, a high frequency of chromosomal non-disjunction, and consequent lethality. Using the same promoter system, we have found that expression of d-box-deleted NimE$^{\text{Cyclin B}}$ results in non-disjunction in addition to its previously reported phenotypes. Our functional characterization of *A. nidulans* group I cyclins provide new insights into cell cycle control mechanisms that are likely to be generally applicable to filamentous ascomycetes.

MATERIALS AND METHODS

Cyclin identification and phylogenetic analyses

To identify putative *A. nidulans* cyclins, we performed BLASTP searches using human, *S. cerevisiae, S. pombe*, and *C. albicans* cyclin protein sequences as queries against the *A. nidulans* FGSC4 protein database (AspGD; www.aspgd.org). We also identified all *A. nidulans* proteins that contained a predicted N-terminal cyclin domain (IPR006671), a C-terminal cyclin domain (IPR004367), a cyclin Pho80-like domain (IPR013922), and/or a cyclin-like domain (IPR013763). Domain predictions were made using InterProScan software from the European Bioinformatics Institute (EBI) and could be found on AspGD's "Domains/Motifs" pages. We then conducted a second round of BLASTP searches, using the putative *A. nidulans* cyclins as queries against 31 filamentous ascomycetes (see Table S2 for a list of the fungi analysed) using NCBI's non-redundant protein database.

Protein sequences were aligned with MAFFT using the L-INS-i method and the Blosum62 matrix (Katoh *et al.* 2017). Maximum likelihood analysis was done in RAxML v8.2.10 (Stamatakis 2014) using the rapid bootstrapping (-f a) algorithm with 1 000 bootstrap replicates under the PROTCAT + Auto (automatically chooses the best protein substitution matrix with respect to the likelihood). RAxML analyses were performed using the free computational resource CIPRES Science Gateway (Miller *et al.*

2010). Phylogenetic trees were visualized in iTOL (Letunic & Bork 2016).

Strains and media

A list of strains used in this study along with their genotypes is given in Table S1. YG (5 g/L yeast extract, 20 g/L D-glucose), supplemented with 400 µL/L of trace element solution (Vishniac & Santer 1957) was used as a liquid complete medium and YAG (YG plus 15 g/L agar) was used as a solid complete medium. As yeast extract does not provide enough riboflavin to fully supplement the *riboB*2 mutation or enough pyrimidines to supplement the *pyrG*89 mutation, the following were added to YAG if needed: riboflavin (2.5 µg/mL), uridine (2.442 mg/mL), and uracil (1 mg/mL). Liquid minimal medium (MM) for imaging consisted of 6 g/L $NaNO_3$, 0.52 g/L KCl, 0.52 g/L $MgSO_4 \cdot 7H_2O$, 1.52 g/L KH_2PO_4, 10 g/L D-glucose, 400 µL/L of trace element solution (Vishniac & Santer 1957) and any additional nutrients required to supplement mutations. For solid MM, the same components as liquid MM plus 15 g/L agar was used. Solid medium utilized for plating protoplasts after transformation required either 342.3 g/L sucrose or 44.7 g/L KCl. pH was adjusted to 6.0–6.5.

The *alcA* promoter [*alcA*(p)] is repressed by glucose and induced by several compounds, one of which is threonine. For our experiments, we repressed the *alcA*(p) with complete medium (e.g. YAG) and for induction we used MM in which the D-glucose was replaced with 9 g/L fructose plus 6.25 mM threonine. The *nmtA* promoter [*nmtA*(p)] is strongly repressed by thiamine, which is present in complete medium (e.g. YAG). Repression experiments with the *nmtA* promoter were, thus, carried out in minimal media with the concentrations of thiamine specified in the text.

Gene targeting and transformation

Linear DNA constructs for transformation of *A. nidulans* were generated by fusion PCR as previously described (Yang *et al.* 2004, Yu *et al.* 2004, Zarrin *et al.* 2005, Nayak *et al.* 2006, Szewczyk *et al.* 2006, Oakley *et al.* 2012). Generation of a fusion PCR product for deleting *pucA* or *clbA* followed the procedure given in Szewczyk *et al.* (2006) as modified by Oakley *et al.* (2012). Q5 Hot Start High Fidelity 2X Master Mix (New England Biolabs) or Phusion (New England Biolabs) DNA polymerases were used for initial amplifications and for fusion PCR.

To create C-terminal fluorescent fusion proteins, the transforming molecules consisted of ~1 000-bp of the C-terminal coding sequence of the target protein (using primers to remove the stop codon) fused in frame to a 30-bp glycine-alanine (GA) linker (Yang *et al.* 2004), which was, in turn, fused in frame with the fluorescent protein coding sequence. The fluorescent protein coding sequence was followed by a 3′ untranslated region from *Aspergillus fumigatus* and a selectable marker [the *A. fumigatus pyrG* gene (*AfpyrG*), *riboB* gene (*AfriboB*) or *pyroA* gene (*AfpyroA*)] and a ~1 000-bp sequence downstream of the target gene. The GFP variant we used in our experiments was a plant-adapted GFP (Fernandez-Abalos *et al.* 1998). The mCherry sequence was the original version described by Shaner *et al.* (2004), and the mRFP variant was as previously described (Campbell *et al.* 2002, Toews *et al.* 2004). The mCherry and tdTomato clones were a gift from Dr. Roger Tsien. pBAD24-sfGFPx1 was a gift from Sankar Adhya & Francisco Malagon (Addgene plasmid # 51558) and pBAD-mTagBFP2 was a gift from Vladislav Verkhusha (Addgene plasmid # 34632). We found that mTagBFP2 was superior to T-Sapphire because it was brighter and the emission spectrum did not overlap with GFP. This allowed it to be distinguished easily from GFP in strains expressing proteins tagged with both fluorescent proteins. A strain carrying An-Nup49-mCherry was provided by C. De Souza and S. Osmani (The Ohio State University, Columbus, OH). The *A. fumigatus riboB* gene used for the mTagBFP2 construct was amplified by PCR from genomic DNA provided by S. Earl Kang, Jr. and Dr. Michelle Momany (The University of Georgia, Athens, GA). *Aspergillus terreus pyrG* and *riboB* genes (*AtpyrG* and *AtriboB*) were amplified by PCR from genomic DNA supplied by Dr. Kenneth Bruno (Pacific Northwest National Laboratory) and further details on those selectable markers were recently published (Dohn *et al.* 2018) and they are available from the Fungal Genetics Stock Center and from Addgene.

The dbΔ-NimE$^{\text{Cyclin B}}$ construct was created as previously described (Nayak *et al.* 2010). The two truncated forms of ClbA were generated as follows. A fragment of the *clbA* gene extending from nucleotide 342 to the end of the gene (nucleotide 2156) was amplified by PCR to generate db1Δ-ClbA. This fragment excludes the N-terminal 60 amino acids that contain the first putative destruction box (RAAFGDVSN). A second fragment of the *clbA gene* extending from nucleotide 603 to the end of the gene (nucleotide 2156) was amplified by PCR to generate db2Δ-ClbA. This fragment excludes the N-terminal 147 amino acids that contain both the first and second (RKTLNKRAT) putative destruction boxes. The primers used to amplify these fragments were designed with a tail at the 5′ end that would anneal to either the *alcA* or the *nmtA* promoter, including a start codon, and a tail at the 3′ end that would anneal to either the GA-GFP cassette or to the selectable marker. The complete transforming molecules of d-box-deleted ClbA or NimE$^{\text{Cyclin B}}$ under the control of either *alcA*(p) or *nmtA*(p) at the *wA* locus consisted of the following: ~1 000-bp of 5′UTR from the *wA* gene, 400-bp of *alcA*(p) or 761-bp of *nmtA*(p), d-box-deleted ClbA or NimE$^{\text{Cyclin B}}$, GA linker + GFP if desired, a 3′ untranslated region from *A. fumigatus,* a selectable marker (either *AfpyrG* or *AfpyroA*), and ~1 000-bp of 3′UTR from the *wA* gene. A similar strategy was used to generate full length ClbA and NimE$^{\text{Cyclin B}}$ (with and without a C-terminal fusion to GA-GFP) under control of the *alcA*(p) or *nmtA*(p) at the *wA* locus.

PCR products were purified using the QIAQuick PCR Purification Kit (Qiagen) or the Monarch PCR & DNA Cleanup Kit (NEB) and analysed by agarose gel electrophoresis. Protoplast formation, purification, and transformation were carried out as described in Szewczyk *et al.* (2006) and Oakley *et al.* (2012). Recipient strains carried *nkuA*Δ to minimize non-homologous end-joining (Nayak *et al.* 2006).

Verification of transformants

Genomic DNA was prepared from transformants using a mini-prep procedure (Edgerton-Morgan & Oakley 2012). Conidia were collected from the surface of a colony using a toothpick or loop and suspended in 50 µL TE buffer (10 mM Tris-HCl, pH 7.5, and 1 mM EDTA) in a microcentrifuge tube. Approximately 50 µL of acid-washed, 425–600 µm glass beads (Sigma) were added and the tube vortexed for 2 min. 2 µL of this solution was immediately

removed and added to 18 µL of TE. 2 µL of this 1:10 solution was used for diagnostic PCR using OneTaq Hot Start Quick-Load 2X Master Mix with Standard Buffer (New England Biolabs, Inc.) according to the manufacturer's instructions. Correct gene integration in each transformant was verified by at least two diagnostic PCR amplifications using different primer pairs: (i) primers outside the target region and (ii) one outside primer and one primer inside the selectable marker.

Microscopy

For imaging, conidia were cultured in 400 µL of liquid MM in eight-chambered cover glasses (Lab-Tek; Thermo Fisher Scientific) with necessary supplements to complement nutritional markers. In some experiments, germlings were fixed in the wells by removing the liquid medium and adding 400 µL of fixative solution [8 % formaldehyde in 50 mM piperazine-N,N′-bis(2-ethanesulfonic acid) (PIPES), pH 6.7; 25 mM EGTA, pH 7.0; 5 mM $MgSO_4$; and 5 % DMSO, pre-warmed to the culture temperature] for 20 min at 37 °C or 30 min at 30 °C. The fixative solution was then removed and replaced with 400 µL Calcofluor White staining solution. For DAPI experiments, 5 × 10^7 conidia were grown in 10 mL liquid media plus 0.1 % agar (to minimize clumping of germlings) at 30 °C at 140 rpm for 12 h. Samples (900 µL) were added to 100 µL of 10 % glutaraldehyde (Electron Microscopy Sciences, Fort Washington, PA), which was previously equilibrated to the culture temperature. They were fixed for 10 min at the culture temperature, spun down for 3 min at 15,500 × g, and then washed 2 × 10 min in double distilled water at room temperature. Samples were resuspended in 0.015 µg/mL DAPI solution.

Two systems, both with environmental chambers to maintain stable temperatures, were used for imaging. The first system was an Olympus IX71 inverted microscope equipped with a mercury illumination source along with Prior shutters, filter wheels, Z-axis drives, and an ORCA ERAG camera (Hamamatsu Photonics). Images were collected with an Olympus 60X/1.42 numerical aperture Plan Apo objective. Filter sets used were a GFP/DsRed2X2M-B dual-band Sedat filter set (Semrock) with a 459–481 nm bandpass excitation filter for GFP, a 546–566 nm excitation filter for mCherry and mRFP, a dual reflection band dichroic (457–480 nm and 542–565 nm reflection bands, 500–529 and 584–679 nm transmission bands), a 499–529 nm emission filter for GFP and a 580–654 nm emission filter for mCherry/mRFP. The second system was an UltraView VoX spinning disk confocal system (PerkinElmer) mounted on an Olympus IX71 inverted microscope. This system was equipped with a software-controlled piezoelectric stage for rapid Z-axis movement. Images were collected using a 60X/1.42 numerical aperture Plan Apo objective (some images taken with a 1.6× Optovar) and an ORCA ERAG camera (Hamamatsu Photonics). Solid state 405-, 488-, and 561-nm lasers were used for excitation and fluorochrome-specific emission filters were used to prevent emission bleed through between fluorochromes. Both systems were controlled by Volocity software (PerkinElmer) running on Power Mac computers (Apple). Magnifications were calibrated with a stage micrometer. Images were exported directly from Volocity after adjustment of minimum and maximum intensity levels (black and white levels) for each channel. Figures were prepared from exported images using Pages (Apple) with no further adjustments.

RESULTS

Phylogenetic analyses of cyclins in aspergilli and other filamentous ascomycetes

Identification of the cyclin repertoire of A. nidulans

Phylogenetic analyses of cyclins have recently been carried out on a variety of different organisms including the model yeasts *S. cerevisiae* and *S. pombe* (Ma *et al.* 2013, Cao *et al.* 2014). However, these evolutionary studies focused on cyclins with an N-terminal cyclin domain, which omits several fungal cyclins. These fungal cyclins do not have an N-terminal cyclin domain but instead have either a cyclin-like or cyclin pho80-like domain (Supplementary Spreadsheet, Tab 1 titled "Cyclins in Anid & Yeasts"). To ensure that we identified all putative cyclins in *A. nidulans,* we utilized two methods: (1) BLASTP searches of the *Aspergillus* genome database (AspGD) using the published amino acid sequences of human, *S. cerevisiae, S. pombe,* and *C. albicans* cyclins and (2) using the InterProScan protein motif search tool to identify all *A. nidulans* proteins that contain an N-terminal cyclin domain (IPR006671), a C-terminal cyclin domain (IPR004367), a cyclin Pho80-like domain (IPR013922), and/or a cyclin-like domain (IPR013763). The cyclin-like domain is also present in the transcription factors TFIIB and TFIIB-related Brf1 which are conserved in fungi.

We determined that the *A. nidulans* genome encodes fifteen putative cyclins (Fig. 1A) of which only six had been previously characterized. Two additional proteins that contain a cyclin-like domain were identified, but they are strong homologs of human TFIIB (AN4928, E-value of 9e-54) and TFIIB-related Brf1 (AN3116, E-value of 4e-68) and are unlikely to be cyclins. Based on both sequence similarity and our phylogenetic analyses, cyclins in fungi fall into three major groups, consistent with previous cyclin family analyses (Ma *et al.* 2013, Cao *et al.* 2014). These results are summarized in Fig. 1A, Table S2, and in the Supplementary Spreadsheet (particularly Tab 1, Table 1 of the Supplementary Spreadsheet).

The complement of cyclins is highly conserved in filamentous ascomycetes

We conducted BLASTP searches of the NCBI protein database for cyclins in the 31 filamentous ascomycetes analysed in de Vries *et al.* (2017) using the amino acid sequences of *A. nidulans* cyclins as a query. The most striking (and perhaps surprising) result of these analyses was the degree of conservation among cyclins, not just in the *Aspergillus* species, but also in the other species which are phylogenetically diverse. In most of the fungi analysed, we identified a single, strong homolog of each of the fifteen cyclins present in *A. nidulans.* A few absences, which may, in part, be due to annotation errors and incidents of gene duplication were also observed (discussed below). The results of the BLASTP searches are summarized in Table S2.

Consistent with previous work, our phylogenetic analyses of all putative cyclins from the 32 species, including *A. nidulans*, indicate that the cyclins fall into three major groups (Supplementary Spreadsheet, Tabs 2–6). The cyclins in group I are the most highly conserved of the three groups based on E-value, query coverage, and the lack of any gene duplications or absences. All species we analysed have three identifiable group I cyclins. They fall into two groups that we designate Cln-like and

A

Species	Group I		Group II						Group III				Total
	Cln-like	B-type	PCL 1,2,9-like	PCL 5-like	Clg1-like	Pho80-like	PCL 6,7-like	PCL 8,10-like	C-like	H-like	L-like	T/K-like	
Saccharomyces cerevisiae	3	6	3	1	1	1	2	2	1	1	-	2	23
Schizosaccharomyces pombe	1	4	-	1	1	-	1	-	1	1	1	2	13*
Candida albicans	3	2	2	1	1	1	1	1	1	1	-	2	16
Aspergillus nidulans	**1**	**2**	**1**	**1**	**2**	**1**	**1**	**1**	**1**	**1**	**1**	**2**	**15**

B

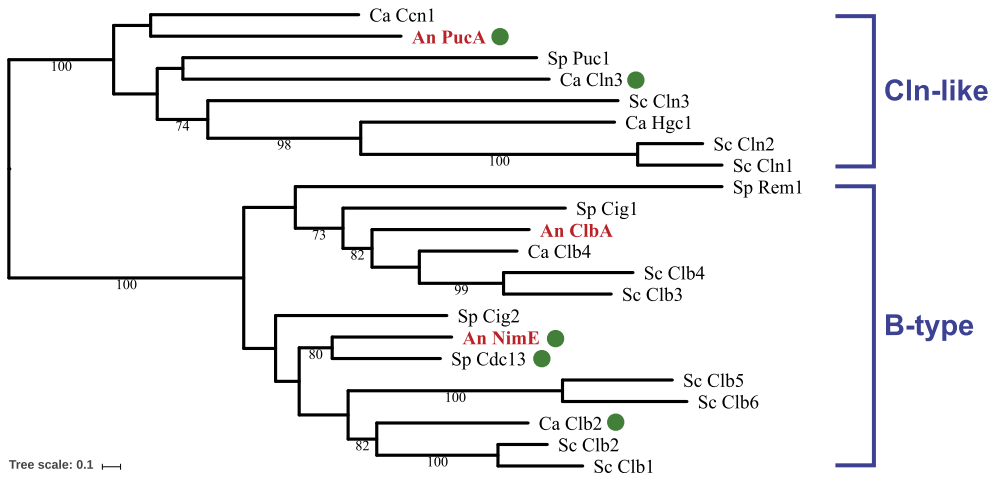

Fig. 1. Cyclin complements of model yeasts and *A. nidulans* A. Table summarizing the number of cyclins in group I, group II, and group III of three model yeasts (*S. cerevisiae, S. pombe,* and *C. albicans*) and in the filamentous fungus *A. nidulans* (bold, red font). Cyclin subfamilies within each group are also shown. The total number of cyclins are displayed at the far right. **S. pombe* has two additional proteins with cyclin-like domains that do not have sequence similarity to other fungal cyclins. See the Supplementary Spreadsheet (Tab 1 and 2) for additional details. **B.** Midpoint-rooted maximum-likelihood phylogenetic tree of group I cyclins in *A. nidulans* (An), *S. cerevisiae* (Sc), *S. pombe* (Sp), and *C. albicans* (Ca). Fungal group I cyclins cluster into two subfamilies, which are indicated in blue font. The abbreviated name of the fungal organism (e.g. An) is followed by the protein name. Cyclins that have been published as essential, or that we have determined are essential in this work, have green dots to the right of their name. Branch support values (70–100 % bootstrap support) are displayed on the branches.

B-type. The B-type cyclins further fall into two well-separated clades. The group I cyclins from filamentous ascomycetes, thus, fall into three clades with each fungus having a single member of each clade. The *A. nidulans* members of the three clades are PucA, NimE$^{Cyclin\ B}$, and ClbA (Supplementary Spreadsheet, Tab 4 titled "FilFungi Group I Cyclins").

The *A. nidulans* group II cyclins do not share strong sequence homology with either group I or group III cyclins, and they only appeared as "hits" when we conducted BLASTP searches using the model yeasts group II cyclins as queries (Supplementary Spreadsheet, Tab 2 titled "Anid vs Model Yeasts Cyclins"). The majority of the species in our study have seven group II cyclins that are strong homologs of the seven *A. nidulans* group II cyclins (Supplementary Spreadsheet, Tab 5 titled "FilFungi Group II Cyclins"). We also observed two subfamilies (Pcl1,2 and Pho80 subfamilies) similar to those observed in *S. cerevisiae*. However, some evidence of gene duplications was observed with group II cyclins. For example, we found that both *Penicillium chrysogenus* and *P. rubens* have three PclA-like proteins and three Pho80-like proteins while *P. digitatum* has only one copy of each. There are three species with only six group II cyclins, all of which were lacking one member of the Pho80 subfamily. However, the missing cyclins could be due to missing or inaccurate annotations.

The group III cyclins in *A. nidulans* also do not share strong sequence similarities with either group I or group II cyclins (Supplementary Spreadsheet, Tab 2 titled "Anid vs Model Yeasts Cyclins"). They are easily detected in BLASTP searches, however, using group III cyclins from yeasts as queries. Group III cyclins are well-conserved in the species in our study. The majority of the species analysed have only five group III cyclins and they are strong homologs of the *A. nidulans* group III cyclins (Supplementary Spreadsheet, Tab 6 titled "FilFungi Group III Cyclins"). Only four species have four instead of five cyclins, but in at least three of the four cases, another sequenced strain of the same species has all five cyclins so the apparent absence may simply be due to sequencing or annotation error. We did not observe any gene duplications in this group.

Model yeasts and filamentous ascomycetes contain different complements of cyclins

The yeasts *S. cerevisiae* and *S. pombe*, have been instrumental in revealing the general principles of cell cycle regulation. The pathogenic fungus *C. albicans* has also been studied extensively because of its significance as a pathogen. We will refer to *C. albicans* as a yeast, although it is dimorphic and has both yeast and filamentous phases. Since these are well-studied ascomycetes, one might expect that they would be good models for understanding cyclin function in aspergilli and other filamentous ascomycetes. These model yeasts are quite phylogenetically distant, however, from the aspergilli and other members of the Pezizomycotina which make up the great

majority of filamentous ascomycetes. The sole filamentous ascomycete in which the functions of group I cyclins have been studied at some depth is *Ashbya gossypii.* This species is a member of the Saccharomycotina, however, and is thus closely related to *S. cerevisiae* and related yeasts and quite distant, phylogenetically, from the great majority of filamentous ascomycetes (Wang *et al.* 2009).

Our analyses reveal that the complement of cyclins in the fungi in our study is significantly different from those of *S. cerevisiae, S. pombe* and *C. albicans*. For simplicity, we will present our comparison of the cyclins of *A. nidulans* to those of these model yeasts, but, as mentioned, *A. nidulans* fairly reflects the complement of cyclins in the other fungi in our study. The sequence homology and phylogenetic relationships between *A. nidulans* and the three model yeasts is shown in the Supplementary Spreadsheet (Tab 2 titled "Anid vs Model Yeasts Cyclins").

With respect to group I cyclins, the most obvious difference between *A. nidulans* and the model yeasts is that whereas *A. nidulans* has only three group one cyclins, *S. cerevisiae, S. pombe* and *C. albicans* have nine, five and five group I cyclins respectively (Fig. 1B). *S. cerevisiae* and *S. pombe* have six and four B-type cyclins respectively whereas *A. nidulans* and *C. albicans* have only two. *S. cerevisiae* and *C. albicans* each have three cln-like cyclins, while *S. pombe* and *A. nidulans* have only a single cln-like cyclin. The multiplicity of cyclins in *S. cerevisiae* may reflect an ancient whole genome duplication (Wolfe & Shields 1997). This may have resulted in functional redundancy accounting for the fact that none of the cyclins are individually essential in this organism. *S. pombe* and *C. albicans* are not thought to have undergone whole genome duplications, and the extra cyclins likely have arisen through individual gene duplications. *A. gossypii* has five group I cyclins, including two cln-like cyclins and three B-type cyclins. One of the two cln-type cyclins is essential and two of the B-type cyclins are essential (Hungerbuehler *et al.* 2007).

The number of group II cyclins varies significantly among model yeasts and differs between the model yeasts and *A. nidulans.* Group II cyclins in the three model yeasts are called Pho85 cyclins (PCLs) after their interacting CDK partner, Pho85. PCLs were first identified and characterized in *S. cerevisiae. S. cerevisiae* has ten PCLs and they separate into two sub-families: the Pcl1,2 subfamily (Pcl1, Pcl2, Pcl5, Pcl9, and Clg1) and the Pho80 subfamily (Pho80, Pcl6, Pcl7, Pcl8, and Pcl10) (Measday *et al.* 1997). *S. pombe* in contrast has only three group II cyclins. *A. nidulans* has seven cyclins, PclA, AN9500, ClgA, AN4984, AN3755, PclB, and Pho80, that cluster with group II cyclins (Fig. 1A, Supplementary Spreadsheet Tab 2) as does *C. albicans.* Although the number is the same, the complement of cyclins in *C. albicans* and *A. nidulans* is significantly different. For example, *C. albicans* has an uncharacterized cyclin (C3_02720W) that has no obvious homolog in *A. nidulans.* In addition, *A. nidulans* has two *clg1*-like genes (*clgA* and an uncharacterized gene AN4984), while *C. albicans* has only one *clg1* gene. Based on the sequence homology and phylogenetic analyses of these four fungi, we observe six major clades of PCL cyclins which we designate as the following, based on the *S. cerevisiae* PCL naming scheme: Pcl1,2,9-like, Pcl5-like, Clg1-like, Pho80-like, Pcl6,7-like, and Pcl8,10-like. The sequence homology and phylogenetic relationship between *A. nidulans* and model yeasts group II cyclins is shown in the Supplementary Spreadsheet (Tab 2 titled "Anid vs Model Yeasts Cyclins").

A. nidulans has five group III cyclins: AN2172 (cyclin C-like), AN2211 (cyclin H-like), AN7719 (cyclin L-like), and PchA and AN10640 (cyclin T/K-like) (Supplementary Spreadsheet, Tabs 1–3). The cyclin C-like and cyclin H-like families are well-conserved with the three model yeasts. However, a cyclin L-like homolog is present only in *A. nidulans* and *S. pombe.*

Functional analysis of Group I cyclins in *A. nidulans*

While it will ultimately be important to characterize all the groups of cyclins in filamentous ascomycetes, the group I cyclins are particularly important because they are key cell cycle regulators. As mentioned above, in the aspergilli and the other fungi in our study they fall into three clades with each fungus having one member of each clade (Supplementary Spreadsheet, Tab 4 titled "FilFungi Group I Cyclins"). This suggests that the group I cyclins are functionally conserved, and that functional information gleaned from one fungus is likely to carry over to many filamentous ascomycetes. Perhaps surprisingly, given the importance of filamentous ascomycetes and the importance of group I cyclins, they have been studied relatively little. The functions of only a single group I cyclin from a member of the aspergilli, $NimE^{Cyclin\ B}$ from *A. nidulans*, has been analysed extensively. A few other group I cyclins from the organisms in our study have been named, but functional analyses have been not been carried out in depth.

$NimE^{Cyclin\ B}$ is an essential B-type cyclin required for both S-phase and mitosis (Bergen *et al.* 1984, O'Connell *et al.* 1992, Nayak *et al.* 2010). Members of the other two clades of group I cyclins have hardly been studied at all in filamentous ascomycetes. We have, consequently, chosen to study the functions of the other two group I cyclins of *A. nidulans,* PucA and the unnamed cyclin encoded by AN2137. PucA was named by De Souza *et al.* (2014) on the basis of similarity to *S. pombe* Puc1 (Pombe unidentified cyclin 1) (E-value of 5e-37), a cyclin that associates with $Cdc2^{Cdk1}$ to regulate the length of G_1 (Martin-Castellanos *et al.* 2000). PucA was found to co-purify with a dual localization-affinity purification (DLAP) tagged version of $NimX^{Cdk1}$. AN2137 has not been characterized at all, nor has it been given a standard *A. nidulans* gene designation. We now designate it *clbA*.

PucA is essential for viability

In order to determine if PucA is essential, we attempted to delete the *pucA* gene (1 312-bp) by transforming the strain LO1516 (genotype listed in Table S1) with a fragment carrying a selectable marker, (*AfpyrG*), flanked by ~1 000-bp *pucA* flanking sequences. When essential genes are deleted in *A. nidulans,* nuclei carrying the null allele are often maintained in heterokaryons spontaneously formed during transformation. Such heterokaryons carry two types of nuclei, parental nuclei and transformed nuclei. Parental nuclei carry a functional copy of the gene under study but do not carry the selectable marker. In transformed nuclei the gene under study has been deleted by replacement with a selectable marker that supports growth on selective media. Such heterokaryons are able to grow on selective media. Importantly, *A. nidulans* conidia are uninculeate, so each conidium carries a parental nucleus or deletant nucleus but not both. The conidia from a heterokaryon carrying a deletion of an essential gene will, thus, not be viable on selective media.

By streaking out conidia from the primary transformants on nutritionally selective media, we can determine if the deleted gene is essential by the presence or absence of growth and colony formation (Osmani *et al.* 1988, Martin *et al.* 1997, Osmani *et al.* 2006). In the case of PucA, multinucleate mycelia transferred to selective media from the primary transformants grew, but conidia from transformants did not grow to form colonies (Fig. 2). This indicates that *pucA* is essential. Diagnostic PCR on DNA prepared from conidia revealed bands diagnostic for both *pucA*Δ and *pucA*+ (data not shown), confirming that the colonies are, indeed, heterokaryons. The fact that the deletion of *pucA* does not block growth in heterokaryons reveals that it is recessive.

PucA is a G_1/S cyclin

PucA has homology to G_1/S cyclins in other organisms, and we hypothesized that the essential function of PucA is to regulate the G_1/S transition. In G_1, the APC/C bound to its activator Cdh1 functions to ubiquitinate S-phase cyclins and other substrates and, thus, targets them for destruction. In order for nuclei to enter S-phase the APC/C-Cdh1 complex must be inactivated by cyclin/CDK complexes (Lukas *et al.* 1999, Sorensen *et al.* 2001, Fukushima *et al.* 2013). CdhA, the *A. nidulans* Cdh1 homolog, has been shown to function similarly to Cdh1 in other organisms by preventing $NimE^{Cyclin\ B}$ accumulation in G_1 (Edgerton-Morgan & Oakley 2012). Previously, we found that the deletion of *cdhA* was not lethal and had little effect on growth, but the length of G_1 was shortened and $NimE^{Cyclin\ B}$-GFP fluorescence started to become visible shortly after mitosis (Edgerton-Morgan & Oakley 2012). If PucA is a G_1/S cyclin involved in the inactivation of CdhA in *A. nidulans*, then the lethality of *pucA*Δ is predicted to be due to failure of inactivation of the APC/C-CdhA complex and consequent blockage of the cell cycle in G_1. If this were the case, deletion of CdhA should allow progression through the cell cycle and enable growth of strains carrying *pucA*Δ. We tested this possibility by attempting to delete *pucA* in a *cdhA*Δ strain (LO2019). We obtained numerous transformants that were viable and could be streaked to single colony (Fig. 5A). Diagnostic PCR revealed that *pucA* was deleted in the transformants (data not shown). Deletion of *pucA* is, thus, not lethal in a *cdhA*Δ background, and this strongly supports the hypothesis that the essential function of *pucA* is to inactivate CdhA at the end of G_1 allowing the accumulation of $NimE^{Cyclin\ B}$ and progression into S phase. Note, however, that the *pucA*Δ, *cdhA*Δ strains grew more slowly than WT or *cdhA*Δ strains and sporulated poorly. This result strongly suggests that *pucA* has non-essential functions, in addition to its essential function in inactivating CdhA, that are important for growth and sporulation.

We used heterokaryon rescue to determine the phenotype of *pucA*Δ in a $cdhA^+$ strain. As mentioned, although *pucA*Δ is lethal in a $cdhA^+$ background, nuclei carrying *pucA*Δ can be maintained in heterokaryons along with nuclei carrying $pucA^+$ and a selectable nutritional marker. The phenotype of *pucA*Δ can then be examined in germinating conidia from the heterokaryon. In the past, we have often used *pyrG*89 as a selectable mutation for heterokaryon rescue. Untransformed spores carrying *pyrG*89 barely germinate on selective media, allowing easy identification of germlings carrying the deletion of interest. We have found, however, that *riboB*2 is an even better selectable marker for heterokaryon rescue. Conidia carrying *riboB*2 swell, but do not extend a germ tube and there is no nuclear division, whereas nuclear division occasionally occurs in *pyrG*89 conidia. It is, thus, easy to distinguish untransformed *riboB*2 conidia among the conidia produced by a heterokaryon. We deleted *pucA* by replacing it with *AtriboB* in strain LO10761, which carries $NimE^{Cyclin\ B}$-GFP as well as An-Nup49-mCherry. Nup49 is a nucleoporin and An-Nup49-mCherry allows visualization of the nuclear envelope. $NimE^{Cyclin\ B}$ accumulates in S phase and if *pucA*Δ prevents inactivation of CdhA, nuclei should be blocked at G_1/S and $NimE^{Cyclin\ B}$ should not accumulate.

We found that An-Nup49-mCherry and $NimE^{Cyclin\ B}$ fluorescence was preserved by a fixation procedure we routinely use and was, in fact, stable for days after fixation. This allowed us to score large numbers of germlings from particular time points

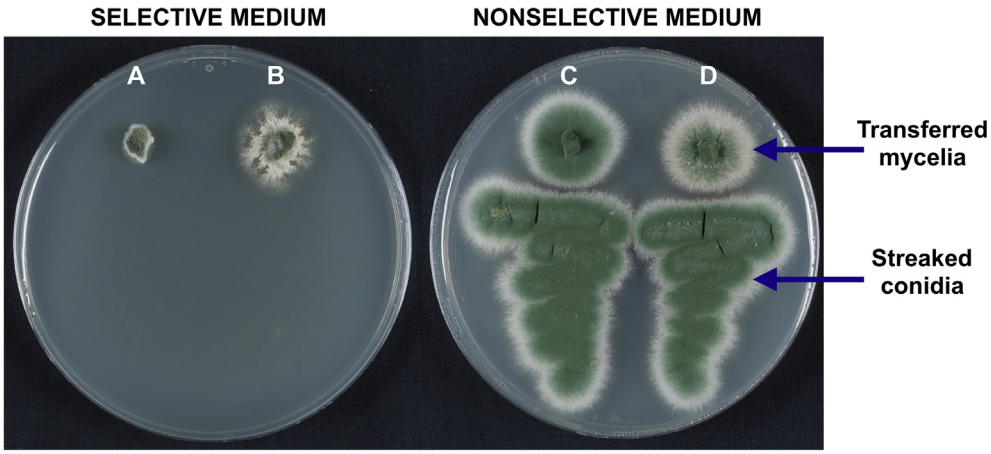

Fig. 2. PucA is an essential cyclin in *A. nidulans*. We used the heterokaryon rescue technique to determine if PucA is essential. A parental, *pyrG*89 auxotrophic strain (LO1516) was transformed with a fragment designed to delete *pucA* (*pucA*Δ) by replacing it with *AfpyrG*. If PucA is essential, conidia carrying *pucA*Δ will not support growth. However, if a heterokaryon is generated during transformation that carries both *pucA*Δ and parental nuclei, hyphae will grow on selective medium (medium lacking uridine and uracil) because parental nuclei provide PucA and transformed nuclei complement *pyrG*89. The conidia produced by the heterokaryon are uninucleate, so they will have either parental nuclei or *pucA*Δ nuclei, and neither will grow on the selective medium. Squares of agar from the parental strain **(A, C)** and a *pucA*Δ transformant heterokaryon **(B, D)** have been placed on the selective medium (left plate) and the nonselective medium (right plate). On the selective medium, hyphae do not grow from the parental square **(A)** but do grow from the transformant, creating a colony with rough edges as is typical for a heterokaryon **(B)**. Conidia have been streaked below each colony. As expected, parental conidia do not grow **(A)**. Crucially, conidia from the transformant colony also do not grow **(B)**, revealing that the transformant is a heterokaryon carrying the lethal deletion *pucA*Δ. The fact that the heterokaryon hyphae grow reveals that *pucA*Δ is recessive. As expected, both hyphae and conidia from the parental strain and the heterokaryon grow on the nonselective medium **(C, D)**.

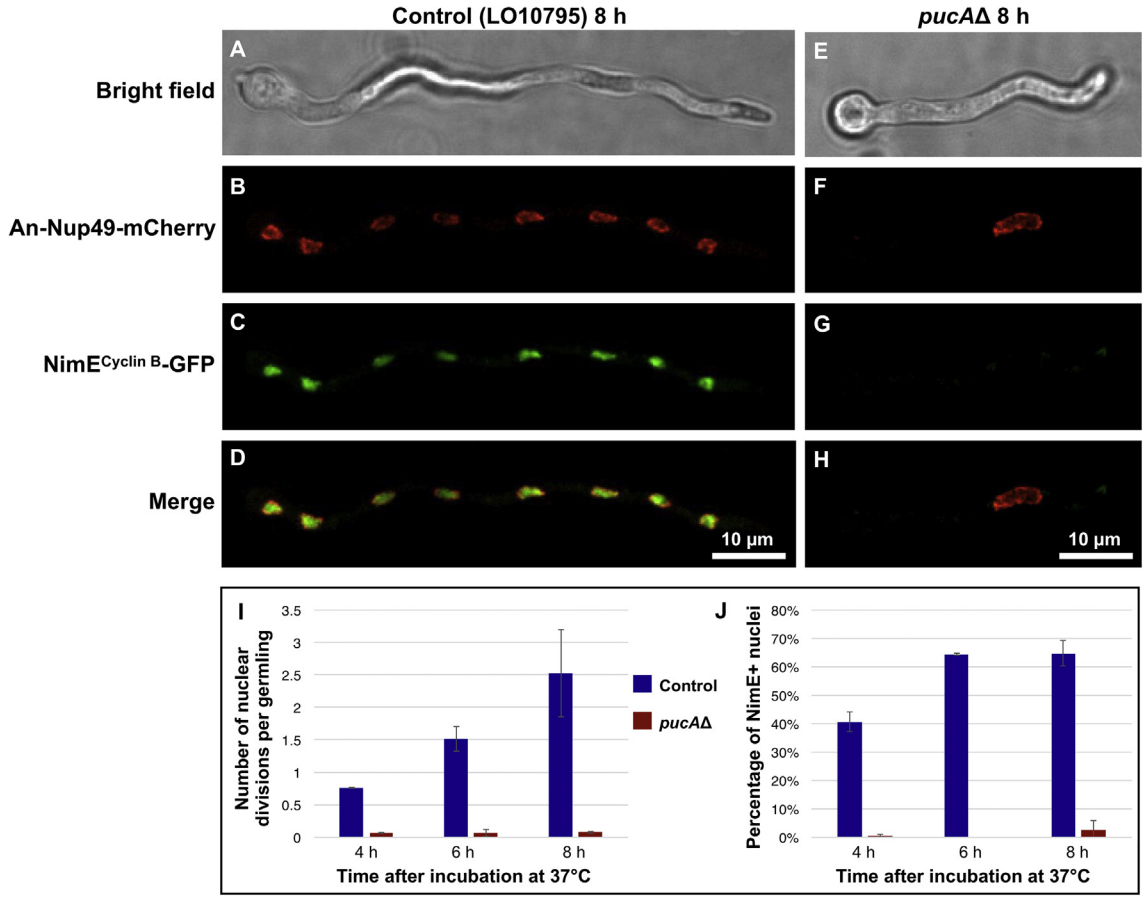

Fig. 3. Deletion of *pucA* blocks cell cycle progression. Bright field images are from a single focal plane (**A, E**) and images **B–D** and **F–H** are maximum intensity projections from Z-series stacks. Images are of a representative control (**A–D**) and *pucA*Δ (**E–H**) germling fixed after 8 h of growth at 37 °C. Three rounds of nuclear division have occurred in the control strain resulting in 8 nuclei. A single nucleus is present in the *pucA*Δ germling, and NimE$^{Cyclin\ B}$-GFP fluorescence is not apparent. (**I**) Very few *pucA*Δ germlings have undergone nuclear division at the 4-, 6-, and 8-h time points, while the control strain has undergone 2–3 rounds of nuclear division by the 8-h time point. (**J**) *pucA*Δ germlings do not accumulate NimE$^{Cyclin\ B}$. Over 100 fixed germlings were imaged and scored at each time point for each of two experiments for both control (strain LO10795) and *pucA*Δ (2 transformants). Error bars indicate mean ± standard deviation of two experiments.

easily. Although the fluorescence was stable, we scored germlings within 24 h of fixation. We separately incubated conidia at 37 °C from two heterokaryons as well as a control strain (LO10795), which was constructed by inserting *AtriboB* at the *yA* locus. We fixed the germlings at 4, 6, and 8 h after inoculation. We collected through-focus Z-series image stacks of random fields and scored germinated conidia for number of nuclei and presence of NimE$^{Cyclin\ B}$. At the 4-h time point, 35.5 ± 0.8 % (2 experiments) of spores had germinated in the control strain. We scored *pucA*Δ germlings at the same time point, realizing that some *pucA*Δ conidia would not have germinated at that time. As Fig. 3 shows, nuclear division was almost completely blocked in the *pucA*Δ germlings. NimE$^{Cyclin\ B}$ accumulation was also almost completely blocked. No NimE$^{Cyclin\ B}$ nuclei were seen at the 4-h time point and less than 1 % of *pucA*Δ nuclei contained NimE-$^{Cyclin\ B}$ at the 6-h and 8-h time points. In the control strain 40.6 ± 3.3 % of nuclei were NimE$^{Cyclin\ B}$ positive at the 4-h time point, 64.4 ± 0.4 % were NimE$^{Cyclin\ B}$ positive at the 6-h time point, and 64.7 ± 4.5 % were NimE$^{Cyclin\ B}$ positive at the 8-h time point (Fig. 3).

Interestingly, the NimE$^{Cyclin\ B}$ positive nuclei in the control strain at the 4-h time point tended to be in germlings with a single nucleus whereas nuclei in binucleate germlings tended to be NimE$^{Cyclin\ B}$ negative. Our interpretation is that the single nuclei were in the first S or G_2 phase after germination and that the binucleate nuclei tended to be in G_1 following mitosis. The percentages of NimE$^{Cyclin\ B}$ positive nuclei at the 6-h and 8-h time points are consistent with our previous observations (Nayak *et al.* 2010, Edgerton-Morgan & Oakley 2012).

These data, in aggregate, reveal that PucA is an essential cyclin that is required for the G_1/S transition and that it functions by inactivating CdhA, and thus the APC/C, and by doing so allows the accumulation of NimE$^{Cyclin\ B}$. Furthermore, this indicates that there are no additional cyclins in *A. nidulans* that are sufficient to inactivate CdhA at the G_1/S boundary and that there are no redundant pathways for CdhA inactivation as has been observed in humans and in *S. cerevisiae* [reviewed in Sivakumar & Gorbsky (2015)].

Deletion of PucA allows nuclear growth but inhibits the DNA replication cycle resulting in nuclei with very diffuse chromatin

To observe nuclear behaviour in a *pucA*Δ strain, we deleted *pucA* in several *cdhA*$^+$ strains carrying different fluorescent proteins, in each case replacing it with *AfriboB.* Since *pucA* is essential in *cdhA*$^+$ strains, we used the heterokaryon rescue technique in all cases and observed the phenotype of *pucA*Δ in germlings that grew from conidia produced by the heterokaryon. We first deleted *pucA* in LO9481, a strain expressing histone H1-T-Sapphire and An-Nup49-mCherry. A control *pucA*+, *riboB*+ strain (LO9537) was constructed by inserting *AfriboB* at the *wA*

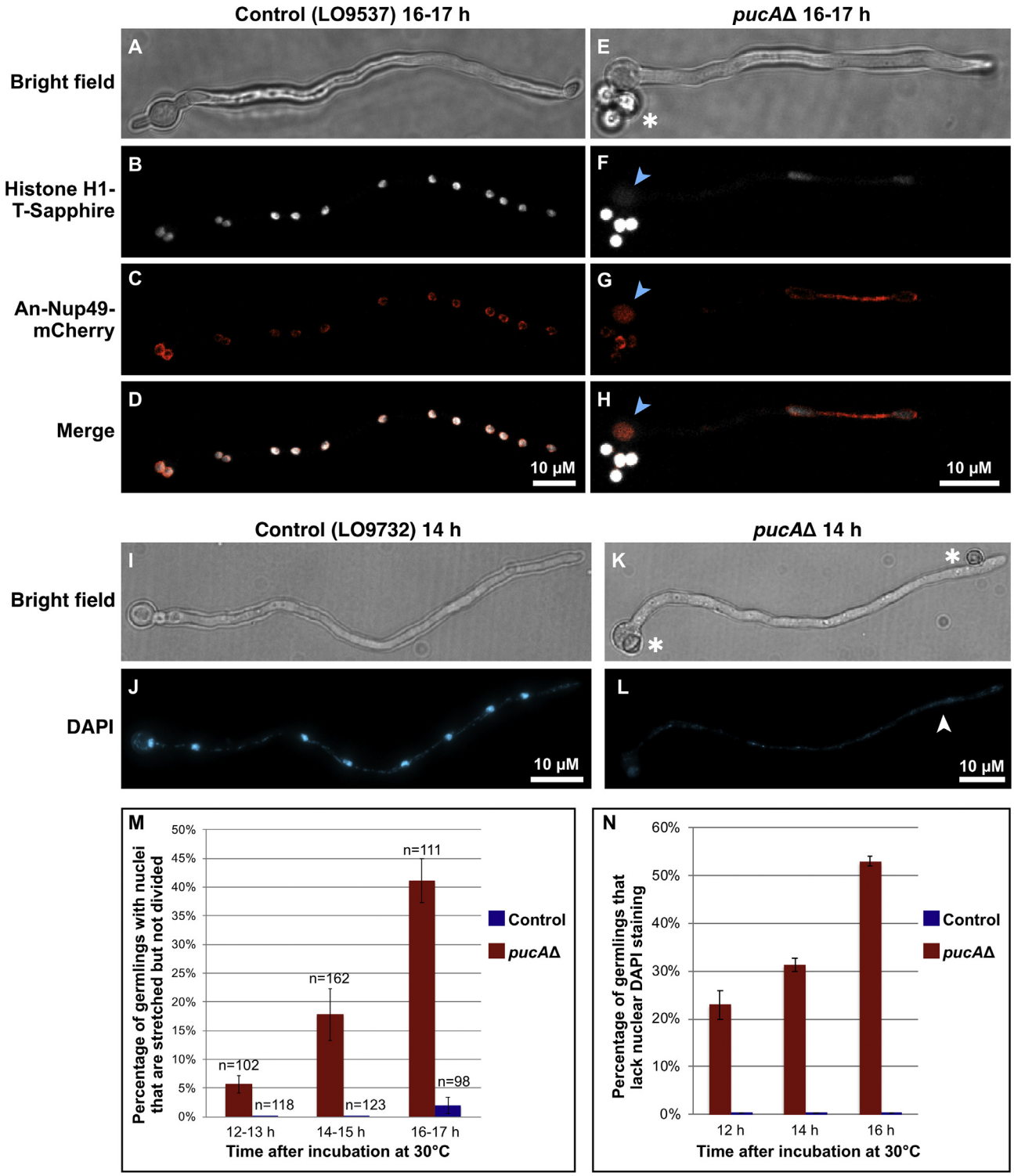

Fig. 4. *pucA*Δ results in stretched nuclei with diffuse DNA and histones. (A–H) Control *pucA*$^{+}$ (LO9537) (**A–D**) and *pucA*Δ (**E–H**) conidia were incubated at 30 °C for 16 h and imaged. Bright field images (**A** and **E**) are single focal plane images, and other images are maximum intensity projections from Z-series stacks. An-Nup49-mCherry allows visualization of the nuclear envelope. The control strain has gone through several cell cycles resulting in many nuclei. The nuclei are normal sized. In the *pucA*Δ germling, however, there is only one large nucleus, and it is extremely stretched as shown by An-Nup49-mCherry fluorescence. There is also faint mCherry and T-Sapphire fluorescence in the vacuole in the conidial swelling of the germling (blue arrowhead in **F–H**). The histone H1 fluorescence in the *pucA*Δ strain is very faint. Note there are four ungerminated parental conidia below the conidial swelling that show bright histone H1-T-Sapphire fluorescence. (**I–L**) DAPI staining of control and *pucA*Δ germlings incubated for 14 h at 30 °C and fixed. **I** and **K** are single focal plane images, and **J** and **L** are maximum intensity projections of Z-series stacks. Nuclear fluorescence is barely visible in **L** even though software was used to increase the brightness level 3.5X in **L** relative to **J**. The arrowhead in **L** points to a possible nucleus. The punctate DAPI staining is mitochondrial DNA. (**M–N**) Control (LO9537) and *pucA*Δ (*pucA*Δ heterokaryon made in parent strain LO9481) conidia containing histone H1-T-Sapphire and An-Nup49-mCherry were grown for 12, 14, and 16 h at 30 °C and then live imaged for one hour at 30 °C. The percentage of germlings with stretched nuclei was scored (**M**); error bars indicate mean ± standard deviation of three separate experiments. n = the number of germlings. Similarly, germlings were scored for the presence of obvious nuclear DAPI staining (**N**); error bars indicate mean ± standard deviation of two experiments (n = 100 germlings per time point). All germlings scored displayed mitochondrial DAPI staining, indicating DAPI staining was successful.

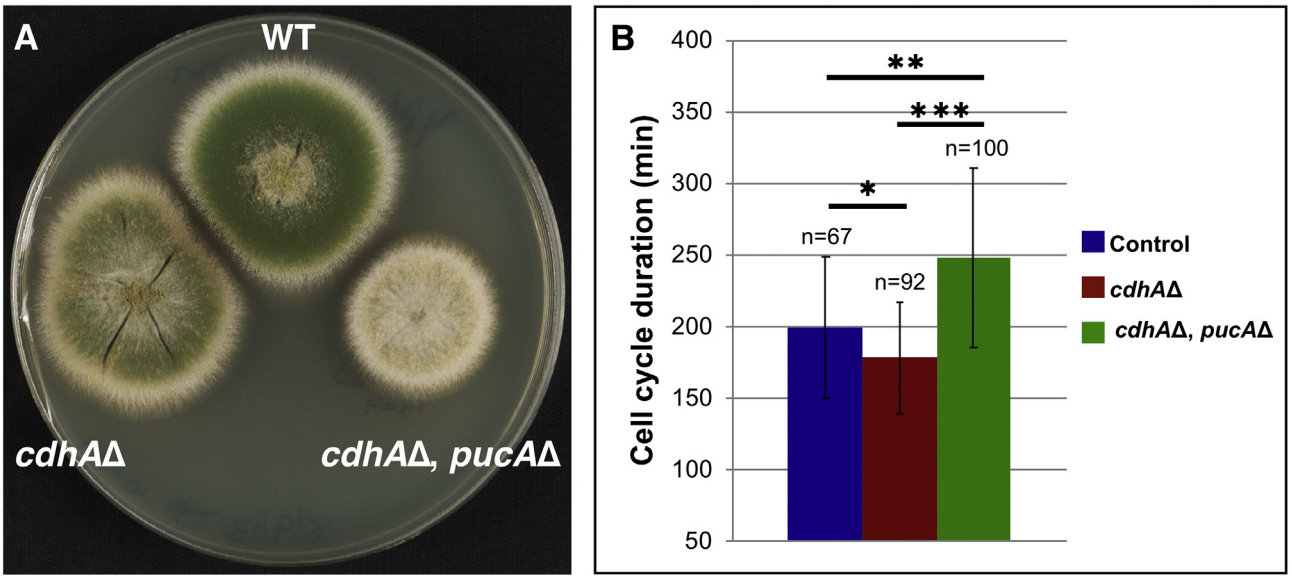

Fig. 5. Deletion of *pucA* in *cdhA*Δ strains is not lethal. (**A**) Strains FGSC4/WT, LO2019, and LO8743 were stabbed on complete medium and incubated at 37 °C for two days. The *pucA*Δ, *cdhA*Δ strain [LO8743 (*cdhA::AfpyrG, pucA::AfpyroA*)] displays reduced growth and sporulation compared to *cdhA*Δ [LO2019 (*cdhA::AfpyrG*)] and WT (FGSC4) strains at all temperatures tested (other temperatures not shown). (**B**) Cell cycle duration was calculated using time-lapse images collected at 10-min intervals of a control (LO1806), *cdhA*Δ (LO2019), and *pucA*Δ, *cdhA*Δ (LO8743) strains, all of which contained histone H1-mRFP. Cell cycle duration was calculated as the time from the end of one mitosis to the end of the next mitosis. Differences in cell cycle duration were statistically significant (* = p value of 0.005, ** = p value of 8e-08, *** = p value of 6e-17). Values are means and error bars indicate standard deviation. n = number of nuclei.

locus in the parent strain LO9481. Conidia from the control strain and from the *pucA*Δ heterokaryon were incubated separately at 30 °C for 12 h at which time both control conidia and *pucA*Δ conidia had germinated. Z-series stacks of random fields were then captured over the next hour. Separate, identically grown samples were also imaged at the 14–15 h and 16–17 h periods. Representative control and *pucA*Δ images at 16–17 h are shown in Fig. 4. Surprisingly, *pucA*Δ germlings at these time points contained either faint or no obvious histone H1-T-Sapphire fluorescence (Fig. 4F). We consistently observed this phenotype in *pucA*Δ germlings from several additional strains with different fluorescent proteins (mRFP and GFP) fused to histone H1 (data not shown). The loss of histone fluorescence is, thus, not due to the T-Sapphire fluorescent protein. We DAPI stained *pucA*Δ and control germlings to determine if there was a loss of DNA fluorescence that parallelled the loss of histone fluorescence. In DAPI stained control germlings, nuclear and mitochondrial genomes are visible and easily distinguished from each other. Mitochondrial DNA is visible as faint punctate fluorescence and nuclear DNA is much brighter and occupies a larger volume, and the nucleus has a characteristic shape. DAPI staining of *pucA*Δ germlings (deletion made in parent strain LO9560) revealed a loss of nuclear DNA fluorescence over time, with over 50 % of *pucA*Δ germlings lacking obvious nuclear DAPI staining at the 16-h time point (incubation at 30 °C, 2 experiments, n = 50 germlings per experiment) (Fig. 4I–L, N). Mitochondrial DNA staining was still apparent in all the *pucA*Δ germlings (Fig. 4L), assuring us that the lack of identifiable nuclear DNA staining was not due to failed DAPI staining. Additionally, we DAPI stained a *pucA*$^+$ control strain (LO9732) and *pucA*Δ germlings side-by-side with identical conditions and timing and imaged them on the same day, and all control germlings had visible nuclear and mitochondrial fluorescence. Thus, loss of identifiable nuclear DNA fluorescence over time parallels the loss of histone H1 fluorescence. We should note, however, that as nuclear DNA becomes stretched and fragmented in *pucA*Δ germlings, it may be present, but too faint to image or it might be indistinguishable from mitochondrial DNA.

To help understand this phenomenon we deleted *pucA* in strain LO10761 (which carries An-Nup49-mCherry). Live imaging revealed that *pucA*Δ resulted in nuclei growing to be much larger than control nuclei (Fig. 3B vs F). Upon longer incubation periods, the nuclear envelopes of *pucA*Δ nuclei exhibited varying degrees of invagination and many became stretched (Fig. S1A–F). Two or more spindle-pole bodies (SPBs) attaching to cytoplasmic microtubules might result in forces being applied to nuclei from different directions. This would, in turn, result in nuclear stretching. We were, consequently, curious as to whether deletion of *pucA* blocked nuclei in G_1 but allowed for SPB duplication. We deleted *pucA* in strain LO10066 which carries GFP-alpha-tubulin, HH1-T-Sapphire, and SepK-tdTomato (a SPB marker). *pucA*Δ germlings were incubated at 37 °C for 8 h and then z-series stacks of random fields were captured over the next hour (two separate experiments). At this time point and temperature, control strains have undergone 2–3 rounds of nuclear division. Most *pucA*Δ germlings (35/49) had either a single nucleus or no obvious histone H1 fluorescence and, of these germlings, most (33/35) had a single SPB despite the fact that many of the nuclei were severely stretched (14/33). Scoring germlings with two nuclei was challenging as the faint histone H1 signal made it difficult to determine whether the nuclei were completely separate or still connected. However, of the germlings that we scored as having two nuclei (14/49 germlings), most (11/14) had a single SPB (Fig. S1J). These data indicate that abnormal SPB duplication is not the cause of the stretching we observe. These results also indicate that forces are applied to the nucleus other than through the SPB.

Long-term time-lapse imaging of *pucA*Δ germlings carrying An-Nup49-mCherry and histone H1-GFP (*pucA*Δ heterokaryon made in parent strain LO9775) revealed that, given sufficiently long incubation, some *pucA*Δ germlings would eventually undergo what appeared to be nuclear division (14/23 germlings

imaged for 16–18 h at 37 °C). However, this was difficult to evaluate because determining whether nuclei underwent nuclear division or were simply pulled apart was sometimes challenging. Interestingly, in those *pucA*Δ germlings that did undergo obvious nuclear division, the histone H1 fluorescence would change rapidly from not apparent to brightly visible as the chromatin condensed (Movie S1). These data demonstrate that chromosomes are present in the large *pucA*Δ nuclei even though they are not visible in interphase. Our interpretation is that DNA replication is strongly inhibited by *pucA*Δ but nuclear growth proceeds, and this results in very large nuclei with very diffuse chromatin. Eventually, the *pucA*Δ-induced G_1 block is overcome in some germlings resulting in a form of mitosis, but, even in those germlings it is not clear that the cell cycle proceeded normally from G_1 to M or that mitosis was normal.

Supplementary video related to this article can be found at https://doi.org/10.1016/j.simyco.2018.06.002.

Notably, this diffuse nuclear histone H1 fluorescence phenotype has been described previously for the deletion of the *nimX*^{Cdk1} gene (De Souza *et al.* 2013). NimX^{Cdk1} has been shown to physically interact with both PucA and NimE$^{Cyclin\ B}$ in *A. nidulans* (De Souza *et al.* 2014). It is, thus, possible that the phenotype we observed in *pucA*Δ germlings is caused by a lack of NimX kinase activity due to the absence of its binding partner PucA.

Deletion of pucA in cdhAΔ strains results in an interphase cell cycle delay

The deletion of *pucA* in a *cdhA*Δ strain results in a decrease in growth and sporulation compared to that of the *cdhA*Δ parent (Fig. 5A). This indicates that PucA has non-essential functions in addition to its essential function of inactivating APC/C-CdhA. To determine if the cell cycle time was altered in the double mutant, we generated a strain carrying *pucA*Δ and *cdhA*Δ and expressing histone H1-mRFP (LO8743, LO8744) to allow us to observe nuclear division. The cell cycle duration was calculated using time-lapse images collected at 10-min intervals at 25 °C. The cell cycle durations for control strains (199 ± 49 min) and *cdhA*Δ strains (178 ± 39 min) at 25 °C have been determined previously (Edgerton-Morgan & Oakley 2012). We scored a different control strain (LO10327) and found it has an essentially identical cell cycle time (198 ± 38 min, n = 72 nuclei). Compared to control and *cdhA*Δ strains, the length of the cell cycle was increased in *pucA*Δ, *cdhA*Δ strains (248 ± 63 min, n = 100 nuclei) (Fig. 5B). The increase was statistically significant. The p-value for *pucA*Δ, *cdhA*Δ vs the control strain was 7.76e-8 and for *pucA*Δ, *cdhA*Δ vs *cdhA*Δ the p-value was 5.74e-17 (unpaired Student's *t*-test). The duration of mitosis in the *pucA*Δ, *cdhA*Δ strain at 25 °C (10 ± 2 min, n = 36) was not significantly different from the control strain (9 ± 1 min, n = 40). It follows that the increased cell cycle time in the *pucA*, *cdhA* double deletant was due to a delay in interphase.

Hyphal growth outpaced nuclear replication in *pucA*Δ, *cdhA*Δ germlings, and this resulted in nuclei being spaced far apart. To quantify this, we fixed control (LO10327), *cdhA*Δ (LO2019), and *pucA*Δ, *cdhA*Δ (LO8743) germlings after 20 h of incubation at 25 °C and used Calcofluor White to visualize the hyphal walls. We scored the distances between interphase nuclei in tip cells that could be seen on the same XY plane using Volocity 6.3 software (Perkin-Elmer). We found that nuclei were 14.5 ± 4.4 µm apart in the control strain (n = 100), nuclei were 12.3 ± 4.3 µm apart in the *cdhA*Δ strain (n = 97), whereas nuclei were 22.5 ± 7.1 µm apart in the *pucA*Δ, *cdhA*Δ strain (n = 89). The fact that longer cell cycle times correlate with increased nuclear spacing is expected. However, the degree of increase in nuclear spacing was disproportionate to the increase in the cell cycle time. Comparing the WT to the *cdhA*Δ, *pucA*Δ double deletant, there was a 25 % increase in cell cycle time in the double deletant relative to the WT, but a 55 % increase in internuclear spacing. The double deletant had a 39 % increase in cell cycle time relative to the *cdhA*Δ strain, but an 83 % increase in nuclear spacing. These data suggest that PucA may have a role, as yet undefined, in internuclear spacing in germlings, beyond its effects on the cell cycle. It is also worth noting that inhibition of colonial growth of the *pucA*Δ, *cdhA*Δ strain (Fig. 5A) was disproportionate to the lengthening of the cell cycle in this strain. PucA may, thus, have roles in colonial growth beyond its cell cycle effects and beyond those observable in germlings.

NimE$^{Cyclin\ B}$ is required for both S-phase and entry into mitosis (Morris 1975, Bergen *et al.* 1984). We were curious if PucA had a role in regulating NimE$^{Cyclin\ B}$ accumulation in S and/or G_2 and, if so, whether that was the cause of the interphase delay we observe in *pucA*Δ, *cdhA*Δ mutants. We generated strains containing *pucA*Δ and *cdhA*Δ and expressing NimE$^{Cyclin\ B}$-GFP and histone H1-mRFP (LO10750, LO10751). NimE$^{Cyclin\ B}$-GFP is absent in G_1, becomes visible in early S phase, and remains apparent in G_2. The length of G_1 is proportional to the percentage of interphase nuclei with no visible NimE$^{Cyclin\ B}$-GFP. Previous work from our lab revealed that the mean percentage of tip cells in *cdhA*$^+$ strains that contained visible NimE$^{Cyclin\ B}$-GFP was 60.0 ± 5.4 % compared to 87.2 ± 3.5 % in *cdhA*Δ strains (Edgerton-Morgan and Oakley, 2012). In the *pucA*Δ, *cdhA*Δ double mutant strains (LO10750 and LO10751), we found that 89.2 ± 4.8 % of tip cells contained visible NimE$^{Cyclin\ B}$-GFP (4 experiments, n = 120 tip cells), and this is essentially identical to *pucA*$^+$, *cdhA*Δ strains. Therefore, the lengthened cell cycle in the double mutant does not appear to be due to a delay in NimE$^{Cyclin\ B}$ accumulation. NimE$^{Cyclin\ B}$ localization appeared normal with a clear enrichment of NimE$^{Cyclin\ B}$ at SPBs.

Deletion of pucA in cdhAΔ strains does not increase mitotic defects but causes interphase nuclear abnormalities

To determine if *pucA* has functions in mitosis, we incubated spores from control (LO1806), *cdhA*Δ (LO2019), and *pucA*Δ, *cdhA*Δ (LO8743) strains at 25 °C, captured Z-series image stacks at 3-min intervals and scored the following mitotic errors: 1) failure of nuclei to divide, 2) mitotic delay (abnormally long periods with condensed chromosomes), 3) apparent nuclear division followed by separated chromatin masses coming back together to reform a single nucleus, and 4) abnormal chromosome segregation (Fig. S2). *cdhA*Δ mutants showed an increase in the rate of total mitotic errors (8.5 % of nuclei, n = 177) compared to control (0.94 % of nuclei, n = 106). The percentage, however, of mitotic errors observed in the *pucA*Δ, *cdhA*Δ strain (10 % of nuclei, n = 160) was not significantly different from that observed in *cdhA*Δ. As presented above, we found no significant difference in the length of mitosis in the *pucA*Δ, *cdhA*Δ strain vs control strains. Taken together, our data indicate that *pucA*Δ does not add significantly to the mitotic abnormalities seen with *cdhA*Δ strains.

In the course of looking for mitotic abnormalities, we observed a number of abnormalities in nuclear appearance and behaviour that were rarely or never seen in control strains. Most of these were also seen in *cdhA*Δ strains, but their frequency was enhanced in the *cdhA*Δ, *pucA*Δ strain. These abnormalities included abnormally large nuclei, nuclei that were pulled or stretched visibly (Fig. S2 D, E), and, most strangely, nuclei in which the chromatin partially condensed and decondensed without mitosis occurring (Movie S2). This phenotype of chromatin partially condensing and decondensing happened to individual nuclei within a cell while the chromatin in other nuclei remained decondensed (Fig. S2F, Movie S2). Altogether, these abnormalities were significant in number with 33.6 % of *cdhA*Δ, *pucA*Δ nuclei exhibiting at least one of these abnormalities in the 30 min prior to mitosis and 22.4 % exhibiting them in the 30 min after mitosis. These abnormalities are quantified in Fig. S2. The abnormally large and stretched nuclear phenotypes are notable in that they are also seen in *pucA*Δ, *cdhA*$^{+}$ germlings from heterokaryons. We looked for microtubule abnormalities that might account for the nuclear stretching, but none were evident (results not shown). The untimely chromosomal condensation and decondensation phenotype was never seen in control cells. These data suggest that PucA, possibly in combination with CdhA, has a role in regulating chromosomal condensation, and, more specifically, in preventing untimely chromosomal condensation.

Supplementary video related to this article can be found at https://doi.org/10.1016/j.simyco.2018.06.002.

Attempts to localize PucA

For clarifying the functions of PucA it would obviously be advantageous to observe its localization. We have not been successful in doing so, but we will summarise our efforts here because we believe they are informative. We generated an N-terminal GFP fusion to PucA but our transformation frequency with the fragment was lower than our positive control. Nevertheless, we were able to isolate 40 transformants from two transformations and carry out diagnostic PCR on them. None of the transformants, however, had a correct GFP-*pucA* integration. These data appear to indicate that transformants carrying the correct N-terminal fusion are not viable. We did not, however, obtain heterokaryon transformants as we would have expected if the GFP-*pucA* construct was recessive lethal. Transformants carrying a C-terminal GFP fusion to PucA were viable but no fluorescence signal was observed. It is likely that PucA is present at levels too low to detect and/or that its half-life is too short to allow GFP to fold and become fluorescent before the protein is destroyed (a particular problem with short lived proteins such as cyclins). We tested a fast-folding fluorescent protein, Superfolder GFP (sfGFP) (Malagon 2013), fusing it to PucA and to NimE$^{\text{Cyclin B}}$. We did not see a fluorescent signal for the C-terminal tagged version of PucA with sfGFP. Interestingly, the fluorescent signal for C-terminal tagged NimE$^{\text{Cyclin B}}$ with sfGFP was weaker than the signal from the GFP variant we currently utilize in the lab (Fernandez-Abalos *et al.* 1998), suggesting that the variant we use is superior to sfGFP.

Localization of ClbA (AN2137)

We generated strains that carried ClbA-GFP and histone H1-mRFP (LO10126 and LO10127), and these strains grew as well as WT strains at all temperatures tested (data not shown). Long-term live time-lapse imaging at 37 °C revealed that ClbA-GFP was first detectable as a single dot in the nucleus 23 ± 10 min before mitosis (n = 73). This correlated to 23 % of the cell cycle. G_2 of *A. nidulans* lasts approximately 40 % of the cell cycle at 37 °C (Bergen & Morris 1983), and, thus, ClbA becomes detectable in mid-G_2. Imaging at 1-min intervals revealed that ClbA-GFP began to disappear from most nuclei just prior to chromatin condensation (51/58 nuclei) (Fig. 6A–O'). ClbA-GFP was rarely observed in nuclei during anaphase or telophase, but occasionally we observed faint ClbA-GFP between the separating chromatin masses in anaphase.

The "dot" localization pattern is consistent with localization to the SPB and/or kinetochores (KTs). In *A. nidulans*, the KTs are immediately adjacent to the SPB during interphase, and they do not separate from the SPB except in prometaphase through early anaphase (Yang *et al.* 2004, De Souza *et al.* 2009). To confirm that ClbA-GFP localizes to the SPB and/or KTs, we generated two additional strains that carried ClbA-GFP. Both carried histone H1-mTagBFP2 (Subach *et al.* 2011), but one carried the SPB marker SepK-tdTomato (Xiong & Oakley 2009), while the other carried the KT marker An-Ndc80-mCherry. Interestingly, we noticed that ClbA-GFP and SepK-tdTomato did not fully overlap and instead localized immediately adjacent to each other (Fig. 6 P–R') while ClbA-GFP and An-Ndc80-mCherry did overlap precisely (Fig. 6 S–U').

This result suggests that ClbA localizes to KTs rather than the SPBs. We performed colocalization analysis with Volocity 6.3 software (Perkin-Elmer) using the Costes Pearson's Correlation algorithm (Manders *et al.* 1993, Costes *et al.* 2004, Barlow *et al.* 2010). With this algorithm, higher correlation values indicate more precise 3D co-localization (1.0 = 100 % overlap of signal). In some cases, optical systems can cause an apparent lateral displacement of objects imaged at different wavelengths. To control for this, we imaged microspheres that fluoresce at both GFP and tdTomato/mCherry wavelengths (Molecular Probes' PS-Speck Microscope Point Source Kit) and found a correlation value of 0.905 ± 0.044 (n = 22 microspheres) when using the 488 nm and 561 nm lasers. The high correlation value indicates that the two wavelengths are not shifted significantly in the XY dimension in our system. We found a correlation value of 0.253 ± 0.234 of ClbA-GFP to SepK-tdTomato (n = 86 nuclei, 2 strains LO11067 and LO11068) and a correlation value of 0.761 ± 0.100 of ClbA-GFP to An-Ndc80-mCherry (n = 89 nuclei, 2 strains LO11253 and LO11254). (Note that the same filter set was used to image SepK-tdTomato and An-Ndc80-mCherry.) These data indicate strongly that ClbA localizes to KTs.

ClbA is not essential but destruction of ClbA is required for viability

To determine if *clbA* is essential we deleted it by replacing it with *AfpyrG*. We found that *clbA*Δ strains (LO10129-LO10131) grew like WT strains at all temperatures tested (data not shown).

An important characteristic of group I cyclins is that their destruction is important for their roles in the cell cycle. In this regard, group I cyclins, particularly the B-type cyclins, have motifs called destruction boxes (d-boxes, RXXLXXXXN) that are recognized by the APC/C. They are then ubiquitinated by the APC/C, and this leads to their destruction by the proteasome. The d-boxes are typically near the N-terminus of these cyclins, and truncation of the N-terminus to delete the d-box or boxes results in a cyclin that drives the cell cycle but arrests the cell

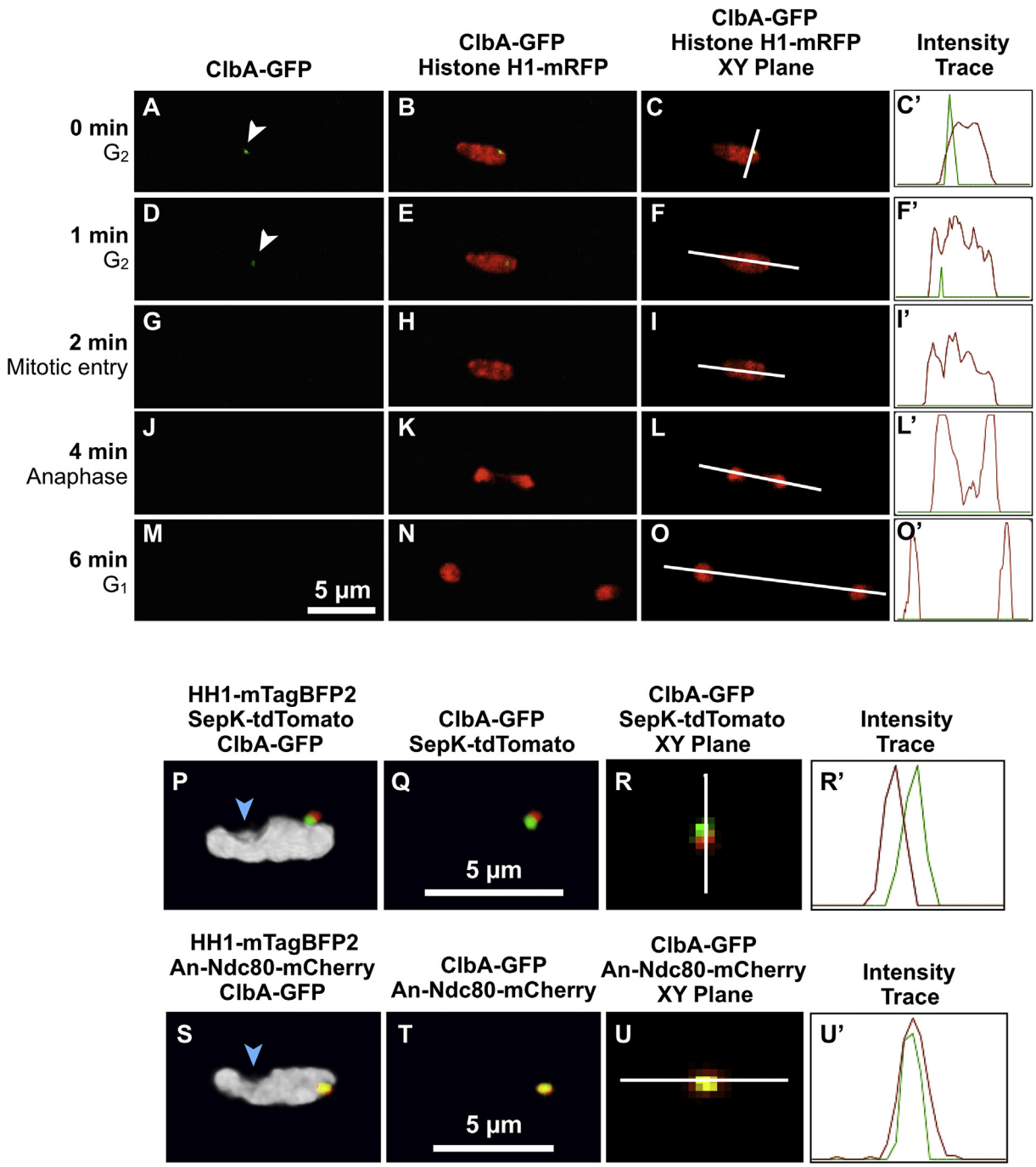

Fig. 6. (A–O') ClbA localizes to kinetochores in G_2 and disappears at mitotic entry. All images were obtained with a spinning disk confocal microscope. T = 0 is in late G_2 and the nucleus transits into mitosis in the following 2 min. Anaphase is underway by 4 min and nuclear division is largely completed by 6 min. The **A–M** and **B–N** columns show maximum intensity projections of Z-series stacks. The **C–O** column shows single focal plane images taken from the same data set, and the **C'–O'** column shows intensity traces over the lines shown in the **C–O** column with ClbA-GFP fluorescence shown in green and histone H1-mRFP shown in red. ClbA-GFP localizes to a dot in the nucleus in G_2 (arrows in **A**, **D)** and disappears during mitotic entry (G). ClbA-GFP is not observed as a dot in the nucleus again until the next G_2. **(P–R')** ClbA-GFP localizes adjacent to the SPB marker SepK. Histone H1-mTagBFP2 is shown in gray, SepK-tdTomato in red, and Clb-GFP in green. **P** and **Q** are three dimensional projections, while **R** is a single focal plane image from the Z-series stack. The minimal overlap is verified by intensity traces in R', which are along the line shown in **R**. The tdTomato trace is shown in red and the GFP trace in green. **(S–U')** ClbA-GFP co-localizes with a kinetochore marker Ndc80. **S** and **T** are three dimensional projections from a Z-series stack with HH1-mTagBFP2 shown in gray, An-Ndc80-mCherry in red and ClbA-GFP in green. **U** is a single focal plane image from the same series. The overlap is verified by intensity traces in the mCherry (red) and GFP (green) channels in **U'** along the line shown in **U**. In **P** and **S** the position of the nucleolus is shown by the absence of histone fluorescence (blue arrows).

cycle at a point at which destruction of the cyclin is required (Murray *et al.* 1989). Removal of the d-box of $NimE^{Cyclin\ B}$, for example, causes a mitotic exit arrest and consequent growth inhibition (De Souza *et al.* 2009, Nayak *et al.* 2010).

ClbA contains two putative d-boxes in its N-terminal region (Fig. 7A). The first putative d-box in ClbA (RAAFGDVSN) is not canonical, but it is almost identical to the $NimE^{Cyclin\ B}$ d-box (RAALGDVSN). The second putative d-box in ClbA (RKTLNKRAT) contains the conserved "RXXL" but not the conserved asparagine at the 9th position. No other identifiable d-box motifs are present in the N-terminus of ClbA. We wished to determine if ClbA d-box motifs play a role in ClbA destruction and, if so, whether destruction of ClbA is important for cell cycle progression.

We created a version of ClbA in which we removed the first d-box (db1Δ-ClbA, eliminating amino acids 2–60) and another

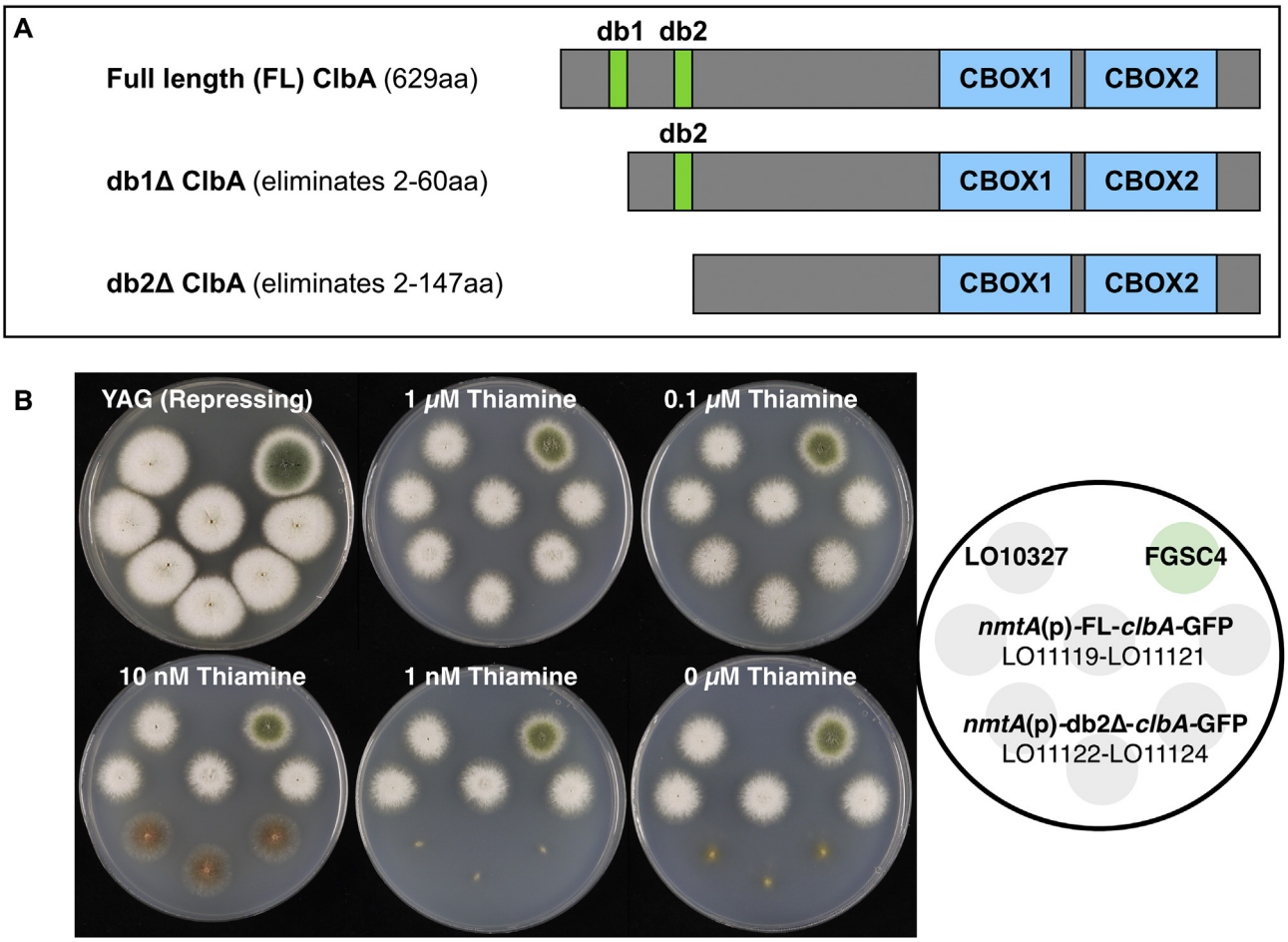

Fig. 7. Inducing expression of full-length and truncated ClbA via the regulatable *nmtA* promoter. A. Diagram of full-length (FL) ClbA with two putative destruction box motifs, db1 (RAAFGDVSN) and db2 (RKTLNKRAT), and two truncated versions of ClbA. CBOX1 designates the first cyclin box fold, also called the N-terminal cyclin domain, and CBOX2 designates the C-terminal cyclin box domain. Constructs shown in **A** were fused to the *nmtA* regulatable promoter and placed at the *wA* locus. **B.** The *nmtA* promoter [*nmtA*(p)] was fused to the N-terminus of both FL-ClbA fused to GFP and truncated (db2Δ) ClbA fused to GFP. These fusion fragments were then placed at the *wA* locus. The endogenous *clbA* gene was not altered in any of the above strains. Three *nmtA*(p)-FL-*clbA*-GFP strains (LO11119-LO11121) grow as well as the control and WT strains (LO10327 and FGSC4) under both repressing (high thiamine) and non-repressing (low or no thiamine) conditions. Three *nmtA*(p)-db2Δ-*clbA*-GFP strains (LO11122-LO11124) grow as well as the WT under repressing conditions (YAG and 1.0 μM thiamine), and grow nearly normally at a thiamine concentration of 0.1 μM. They are extremely sick under partially-repressing conditions (10 nM thiamine) and dead under non-repressing conditions (1.0 nM thiamine or less). Although GFP-tagged strains are shown, identical results were obtained with strains expressing non-GFP-tagged FL ClbA and db2Δ-ClbA.

version in which we deleted the N-terminal region that contained both putative d-boxes (db2Δ-ClbA, eliminating amino acids 2–147) (Fig. 7A). We also created versions of the d-box-deleted ClbA and two d-box-deleted ClbA in which GFP was fused to the C-terminus (db1Δ-ClbA-GFP and db2Δ-ClbA-GFP). We initially placed db1Δ-ClbA, db1Δ-ClbA-GFP, db2Δ-ClbA, db2Δ-ClbA-GFP, full length (FL) ClbA, and FL-ClbA-GFP (separately) under the control of the regulatable *alcA* promoter [*alcA*(p)] at the white (wA) locus in a strain expressing histone H1-mRFP (parental strain LO1516). In these strains, the endogenous *clbA* gene was not altered. On repressing media, all six strains grew like WT and control strains (Fig. S3). On inducing media, the expression of db1Δ-ClbA or db1Δ-ClbA-GFP significantly decreased growth while the expression of db2Δ-ClbA or db2Δ-ClbA-GFP almost completely inhibited growth and sporulation. Induction of expression of FL-ClbA or FL-ClbA-GFP did not alter growth compared to WT strains. Since the endogenous copy of *clbA* was not altered in these strains, these data indicate that destruction of ClbA is essential for viability and that d-box-deleted versions of ClbA act in a dominant negative fashion.

We also wished to determine the phenotype caused by failure of destruction of ClbA. Since the growth phenotypes caused by db2Δ-ClbA expression and db2Δ-ClbA-GFP expression appear to be the same, we have used GFP fusions for the bulk of our experiments, because the GFP allows us to monitor the location of the molecules. We encountered difficulty with the *alcA*(p) due to its "leakiness". While colony growth was normal on *alcA* repressing media (Fig. S3), spore viability was very low in strains carrying the *alcA*(p) driving expression of db2Δ-ClbA or db2Δ-ClbA-GFP even on *alcA*(p) repressing media, making it difficult to determine the phenotype of db2Δ-ClbA-GFP via microscopy. We reasoned that this was due to leakiness of the *alcA*(p) therefore, we searched for a more strongly repressible promoter.

The nmtA promoter can be regulated more effectively than the alcA promoter

In *S. pombe, nmt1* has been shown to be highly transcribed in minimal medium and strongly repressed by the addition of thiamine (Maundrell 1990, Tamm 2012). Our lab had previously analysed the promoter activity of a 761-bp sequence immediately upstream of the *A. nidulans nmt1* homolog *nmtA* (An8009). This 761 bp *nmtA* promoter [*nmtA*(p)] sequence, fused to GFP was placed at the *yA* locus and found to repress GFP fluorescence in

the presence of thiamine and allow constitutive GFP expression in the absence of thiamine.

We placed FL-ClbA-GFP and db2Δ-ClbA-GFP under control of *nmtA*(p) at the *wA* locus in a strain that carries histone H1-mRFP (parental strain LO1516). The endogenous copy of *clbA* was not altered. We found that a thiamine concentration of 0.1 μM repressed *nmtA*(p)-driven expression of db2Δ-ClbA-GFP sufficiently to allow nearly normal growth and 1.0 μM or more was sufficient to allow growth like the WT on solid (Fig.7B) and in liquid medium. These results suggested that *nmtA*(p) can be more strongly repressed than *alcA*(p) and this, in fact, proved to be the case (see results below).

Failure to degrade ClbA results in a mitotic arrest as well as nondisjunction

To determine the phenotype of db2Δ-ClbA-GFP, we collected conidia from strains carrying double d-box-deleted, GFP tagged ClbA, [LO11122 (*nmtA*(p)-db2Δ-*clbA*-GFP)], a strain carrying *clbA*$^{+}$ fused to GFP and under control of *nmtA*(p) [LO11119 (*nmtA*(p)-FL-*clbA*-GFP)], and a control *clbA*$^{+}$ strain (LO10327). The conidia were collected from material grown on solid medium containing a concentration of 0.1 μM thiamine, a concentration that partially represses expression (Fig. 7B). To allow expression from *nmtA*(p), we inoculated these conidia into liquid media without thiamine. We incubated them at 30 °C for ~6 h, and then captured Z-axis image stacks at 10-min intervals for 12 h. We found that LO11122 conidia (*nmtA*(p)-db2Δ-*clbA*-GFP) generated short germ tubes, and, once the cells entered mitosis, they became blocked in mitosis. The mitotically arrested nuclei displayed one or more of the following defects: failure of anaphase A, failure of anaphase B, nondisjunction, or chromatin collapsing back into a single mass after initially separating.

To better quantify these observations, we fixed LO11122, LO11119, and LO10327 germlings after 12 h of growth at 30 °C. At this time and temperature, control germlings (LO10327) had undergone 2.0 ± 0.1 nuclear divisions and contained ~ 4 nuclei (206 germlings scored from 2 separate experiments). Expression of FL-ClbA-GFP from *nmtA*(p) (strain LO11119), in the absence of thiamine, slightly decreased the number of nuclear divisions to 1.8 ± 0.1 (207 germlings scored in 2 separate experiments). FL-ClbA-GFP is predicted to be over expressed in these strains, and this was confirmed by microscopy. This overexpression, however, had a modest effect on the cell cycle, if any. Expression of db2Δ-ClbA-GFP (LO11122), however, drastically reduced the number of nuclear divisions to 0.3 ± 0.1 (180 germlings scored from 2 separate experiments). This indicates that destruction of ClbA is required for nuclear replication. Additionally, we found that chromatin was condensed in 53.8 % ± 3.1 % of germlings in the db2Δ-ClbA-GFP expressing strain (LO11122) nuclei compared to 5.9 % ± 2.1 % in the FL-ClbA-GFP expressing strain (LO11119) and 4.5 ± 1.6 % in the *clbA*$^{+}$ strain (LO10327). These data reveal that expression of db2Δ-ClbA-GFP results in a strong mitotic block.

To determine the nature of the mitotic arrest, we needed to be able to collect Z-series image stacks at short intervals. We found that if we collected LO11122 conidia from solid medium with a concentration of 1.0 μM thiamine and then grew those conidia at 30 °C in liquid media without thiamine, germination and initial growth were normal. Germlings underwent 2–3 rounds of normal nuclear divisions and then began to show mitotic abnormalities and mitotic blockage. This approach allowed us to find and image cells entering mitosis and displaying the phenotypes caused by expression of db2Δ-ClbA-GFP.

Imaging revealed that, as anticipated, little or no of db2Δ-ClbA-GFP was present initially. The absence of db2Δ-ClbA-GFP is almost certainly due to the conidia carrying over enough thiamine to inhibit expression from *nmtA*(p). Upon continued incubation without thiamine, db2Δ-ClbA-GFP began to be visible at KTs. The exact timing of its appearance varied to some extent among germlings, but it generally became detectable between the second and third nuclear divisions. Nuclei often went through one round of mitosis after db2Δ-ClbA-GFP became visible. In these cases, we found that db2Δ-ClbA-GFP was removed from the KTs, and this strongly correlated with mitotic entry. In most cases mitosis appeared normal. Immediately after mitosis, however, db2Δ-ClbA-GFP became visible at KTs (in marked contrast to controls), and db2Δ-ClbA-GFP fluorescence increased markedly through interphase. At the end of this interphase db2Δ-ClbA-GFP left the KTs, nuclei entered mitosis, and a catastrophic mitosis followed (Movie S3, Fig. 8). Full condensation of chromatin was never observed until db2Δ-ClbA-GFP left the KTs (n = 46/46 nuclei, strains LO11122 and LO11123). These data indicate that ClbA is removed from KTs by a mechanism other than simple destruction, and they are consistent with the hypothesis that ClbA must be removed from KTs in order for mitotic entry to occur.

During these catastrophic mitoses, although db2Δ-ClbA-GFP left the KTs at mitotic onset, it was present at higher levels in the nucleoplasm than in the cytoplasm in the majority of nuclei (45/46 nuclei; Fig. 8 F, J). Overexpressed ClbA-GFP or ClbA-GFP driven by its endogenous promoter rapidly disappeared from the nucleoplasm of mitotic nuclei. The vast majority of nuclei in db2Δ-ClbA-GFP germlings entered anaphase (43/46 nuclei; Fig. 8 M–P) relatively quickly after chromosomal condensation but displayed obvious nondisjunction (42/43 nuclei; Fig. 8 M–T). The chromatin in many nuclei eventually collapsed back into one mass (34/43 nuclei) after initially separating in anaphase. This phenotype is consistent with force being exerted on the chromosomes by the mitotic apparatus, causing chromosomal separation but daughter chromatids failing to disjoin from each other and the elasticity of chromatin pulling the chromatids back into a single mass. During these failed anaphase attempts, db2Δ-ClbA-GFP could be seen faintly on the spindle, in the nuclei, and/or at dot(s) in the separating chromatin (46/46 nuclei) (Fig. 8 N–P, R–T). These data, in aggregate indicate that destruction of ClbA is required for chromosomal disjunction.

Supplementary video related to this article can be found at https://doi.org/10.1016/j.simyco.2018.06.002.

Interestingly, we observed that *nmtA*(p)-driven expression of either ClbA-GFP or db2Δ-ClbA-GFP resulted in a GFP signal at septa. This was not observed in strains in which expression of ClbA-GFP was driven by its endogenous promoter, even when the laser and exposure settings were increased to allow imaging of very faint signals (data not shown).

Destruction of NimE$^{Cyclin\ B}$ is important for chromosomal disjunction

Expression of destruction box-deleted NimE$^{Cyclin\ B}$ (dbΔ-NimE-$^{Cyclin\ B}$) also results in a strong mitotic block. dbΔ-NimE$^{Cyclin\ B}$-GFP expressing cells enter mitosis and progress through anaphase before becoming blocked in telophase with dbΔ-

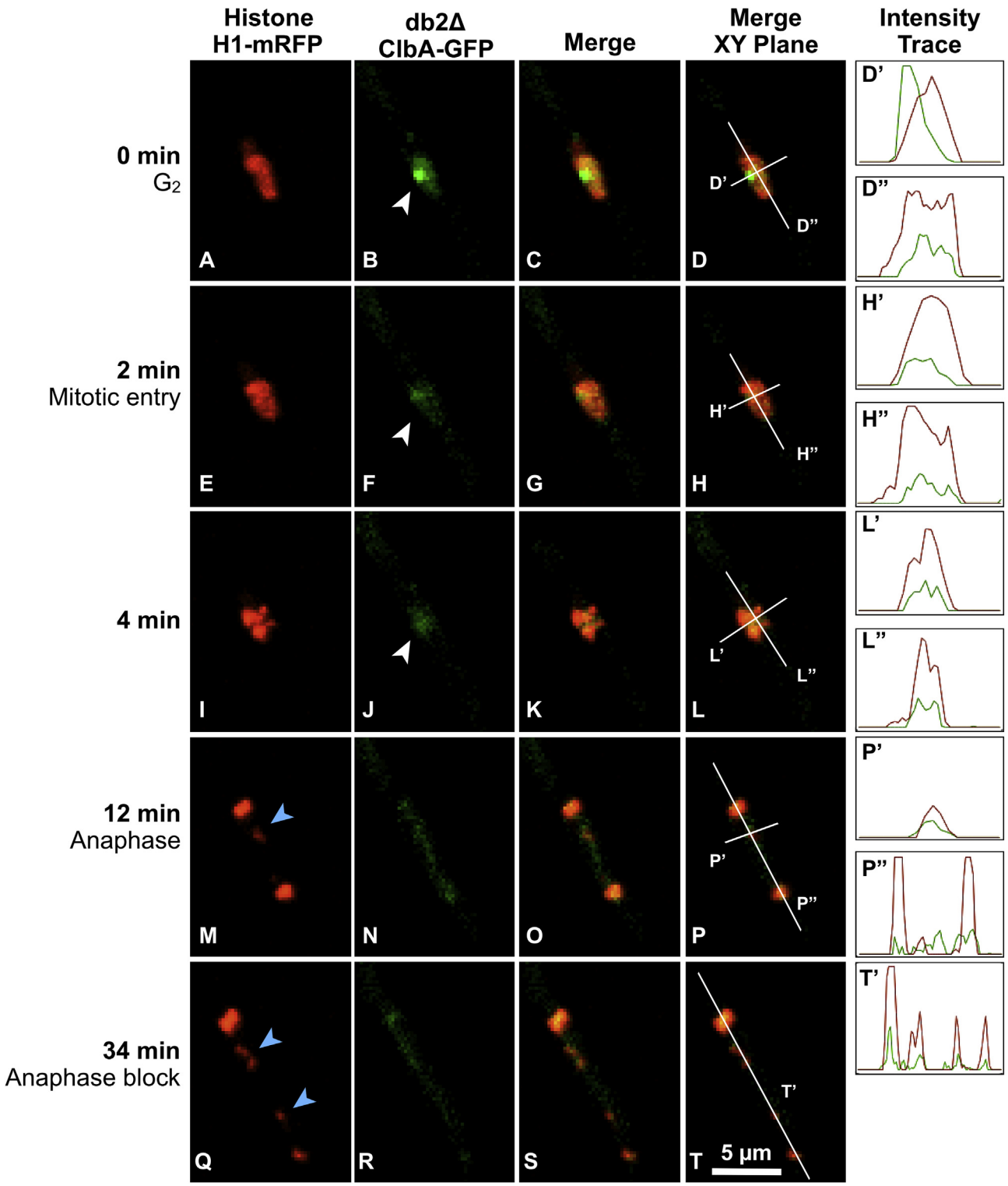

Fig. 8. Expression of db2Δ-ClbA-GFP results in nondisjunction and mitotic arrest in anaphase. Conidia carrying *nmtA*(p)-db2Δ-*clbA*-GFP and histone H1-mRFP (strains LO11122-LO11124) were collected from hyphae growing on media containing 1.0 µM thiamine, incubated at 30 °C for 10–12 h in non-repressing liquid media (i.e. lacking thiamine), and then imaged in 2-min intervals. Images are maximum intensity projections from Z-series stacks. In G_2, db2Δ-ClbA-GFP localizes strongly to the kinetochores (KTs) and faintly to the nucleoplasm (**A–D**). At mitotic entry, db2Δ-ClbA-GFP leaves the KTs but can be seen faintly in the nucleoplasm (**E–H**). Mitosis is stalled or blocked in anaphase, and db2Δ-ClbA-GFP can be seen faintly along the spindle and at a dot in the separating chromatin (**M–T**). White arrows designate db2Δ-ClbA-GFP at the KTs and/or nucleoplasm (**B, F, J**). Blue arrows point to chromosomes that failed to disjoin properly (**M, Q**).

$NimE^{Cyclin\ B}$-GFP remaining at the spindle poles (De Souza *et al.* 2009, Nayak *et al.* 2010). We utilized the same destruction box-deleted cyclin B construct used in previous work (De Souza *et al.* 2009, Nayak *et al.* 2010) fused to GFP (dbΔ-$NimE^{Cyclin\ B}$-GFP) but placed it under the control of the *A. nidulans nmtA* promoter at the *wA* locus (LO11357-LO11359). Our results were consistent with the previously mentioned studies (data not shown). However, when we followed nuclei through mitosis by capturing time-lapse Z-series stacks at one-minute intervals, we also observed a high frequency of nondisjunction in dbΔ-$NimE^{Cyclin\ B}$-GFP expressing cells (19/32 nuclei) (Movie S4), which was not previously reported. Thus, destruction of both ClbA and $NimE^{Cyclin\ B}$ during mitosis is required for proper chromosomal disjunction.

Supplementary video related to this article can be found at https://doi.org/10.1016/j.simyco.2018.06.002.

Cohesin is removed from chromosomes in db2Δ-ClbA and dbΔ-NimE$^{Cyclin\ B}$ expressing strains

The cohesin complex holds sister chromatids together, and its removal is required for chromosomal disjunction. Cohesin complex removal is regulated by mitotic cyclins and the APC/C [reviewed in Wong (2010)]. Failure of cohesin complex removal is, thus, a plausible cause for the high frequencies of non-disjunction caused by db2Δ-ClbA and dbΔ-NimE$^{Cyclin\ B}$. Although the cohesin complex has been studied extensively in other organisms, there is very little information on it in filamentous fungi. To determine if db2Δ-ClbA and dbΔ-NimE$^{Cyclin\ B}$ altered the removal of the cohesin complex, we first had to investigate the localization and removal of the complex in control cells.

The core cohesin complex is composed of Scc1 (also known as Rad21 in humans and Mcd1 in *S. cerevisiae*), Scc3, and two SMC (Structural Maintenance of Chromosomes) proteins called SMC1 and SMC3. The *A. nidulans* homolog of human Rad21 and *S. cerevisiae* Mcd1 is AN7465 (E-value of 2E-29 and 3E-17, respectively), which we now designate *sccA*. Strains carrying SccA-GFP and HH1-mRFP (LO3231) had previously been constructed in our lab. We found that SccA-GFP localizes to nuclei but not nucleoli throughout interphase (arrows in Fig. S4A–C), and, as expected, it leaves the chromatin during mitosis. To narrow down the timing of disappearance of SccA-GFP from chromosomes during mitosis, we captured Z-series image stacks at 1-min intervals (n = 42 nuclei). SccA-GFP localized to condensed chromatin (42/42 nuclei, Fig. S4D–F) early in mitosis but, as expected, disappeared at the beginning of anaphase. In some cases (10/42 nuclei), SccA-GFP was observed between the separating chromatin in early anaphase (Fig. S4G–I, see blue arrow), but this signal always disappeared in late anaphase. After mitosis, SccA-GFP slowly accumulated in nuclei in early G_1, and this signal intensified as the cell cycle progressed.

We next wanted to determine if SccA was removed from chromosomes during mitosis in db2Δ-ClbA and dbΔ-NimE$^{Cyclin\ B}$ expressing cells. We generated strains that carried SccA-GFP, histone H1-mRFP, and either *nmtA*(p)-db2Δ-*clbA* (LO11211) or *nmtA*(p)-dbΔ-*nimE$^{cyclin\ B}$* (LO11217) inserted at the *wA* locus. A control strain (LO11202) that carried SccA-GFP and histone H1-mRFP, was constructed by inserting *AfpyroA* at the *wA* locus. The endogenous *clbA* and *nimE* genes were not altered in any strain. We harvested conidia from each of these strains grown on media with 1.0 μM thiamine. We inoculated conidia into liquid media lacking thiamine (allowing expression of the d-box-deleted cyclins). incubated the cultures at 30 °C for ~6 h, and then captured images of Z-axis stacks at 10-min intervals for 12 h.

Expression of db2Δ-ClbA (Fig. 9) or dbΔ-NimE$^{Cyclin\ B}$ (Fig. S5) led to a mitotic arrest in the second or third nuclear division cycle, as seen in previous experiments. Perhaps surprisingly, we found that SccA-GFP disappeared in all nuclei at anaphase onset in both LO11211 (db2Δ-clbA, n = 31/31 nuclei) and LO11217 (dbΔ-NimE$^{Cyclin\ B}$, n = 38/38 nuclei). We followed these nuclei over long periods of time and found that they stayed in mitosis for a long (although variable) time after cohesin removal/anaphase (the range was 30–300+ min but most were in mitosis more than 1 h). However, eventually SccA-GFP would begin to re-accumulate faintly in condensed nuclei, and the chromosomes of some nuclei would decondense and accumulate SccA-GFP more brightly. Interestingly, we found that mitotic exit did not occur for all nuclei at the same time in the same cell, and some nuclei would remain condensed even if SccA-GFP accumulated (Figs 9P–U, S5P–U). These cells continued to cycle and attempt additional mitoses, and the number of nuclear fragments, likely due to repeated nondisjunction, increased (Figs 9, S5). We also imaged these strains in short, 2-min, intervals and obtained similar results. These data indicate that SccA-GFP is removed from chromosomes during mitosis in cells expressing either db2Δ-ClbA or dbΔ-NimE$^{Cyclin\ B}$ and, thus, failure of cohesin complex removal is not the cause of the failure of chromosomal disjunction we observe.

Expression of db2Δ-ClbA, but not dbΔ-NimE$^{Cyclin\ B}$, extends interphase

Although the mitotic phenotypes caused by expression of db2Δ-ClbA and dbΔ-NimE$^{Cyclin\ B}$ are similar, we found the effects of their expression on cell cycle timing were very different. To examine the effects of db2Δ-ClbA and dbΔ-NimE$^{Cyclin\ B}$ on the cell cycle, we grew strains LO11211 [*nmtA*(p)-db2Δ-*clbA*] and LO11217 [*nmtA*(p)-dbΔ-*nimE$^{cyclin\ B}$*] on 1.0 μM thiamine, harvested spores, and inoculated them into media with no thiamine. As mentioned above, the thiamine is gradually depleted, and the d-box-deleted cyclins become expressed, resulting in a mitotic block. The presence of a mitotic block indicates that the d-box-deleted cyclin was expressed in the previous cell cycle. By timing the cell cycle prior to a mitotic block, we can determine if the d-box-deleted cyclin alters the length of the cell cycle. In LO11202 (control), we found the average cell cycle duration (time in min from the beginning of one mitosis to the beginning of the next mitosis) at 30 °C for the first 3 nuclear divisions was 150 ± 34 min (n = 63 nuclei). In LO11217 [*nmtA*(p)-dbΔ-*nimE-cyclin B*], we found the cell cycle duration was 150 ± 36 (n = 21 nuclei) when followed by a normal mitosis and 155 ± 39 min (n = 35) when followed by an abnormal mitosis. These values were not significantly different from the control. Expression of dbΔ-NimE$^{Cyclin\ B}$, thus, does not significantly alter the length of the cell cycle. LO11211 which expresses db2Δ-ClbA, however, had an average cell cycle time of 183 ± 28 min (n = 49 nuclei) when followed by a normal mitosis and an average cell cycle time of 209 ± 49 min (n = 31 nuclei) when followed by an abnormal mitosis. These were both significantly different from the control ($p < 0.001$). Expression of db2Δ-ClbA, thus, does increase the length of interphase. We attribute the lengthened cell cycle before normal mitosis to the accumulation of a small amount of db2Δ-ClbA at levels insufficient to arrest mitosis as noted above. These data strongly indicate that ClbA has an inhibitory role in cell cycle progression in interphase.

DISCUSSION

Phylogenetic analyses

Given the significance of cyclins in cell cycle regulation and cell growth, there has been surprisingly little study of cyclins in filamentous ascomycetes. We report the identification and phylogenetic analysis of all cyclin domain-containing proteins in the

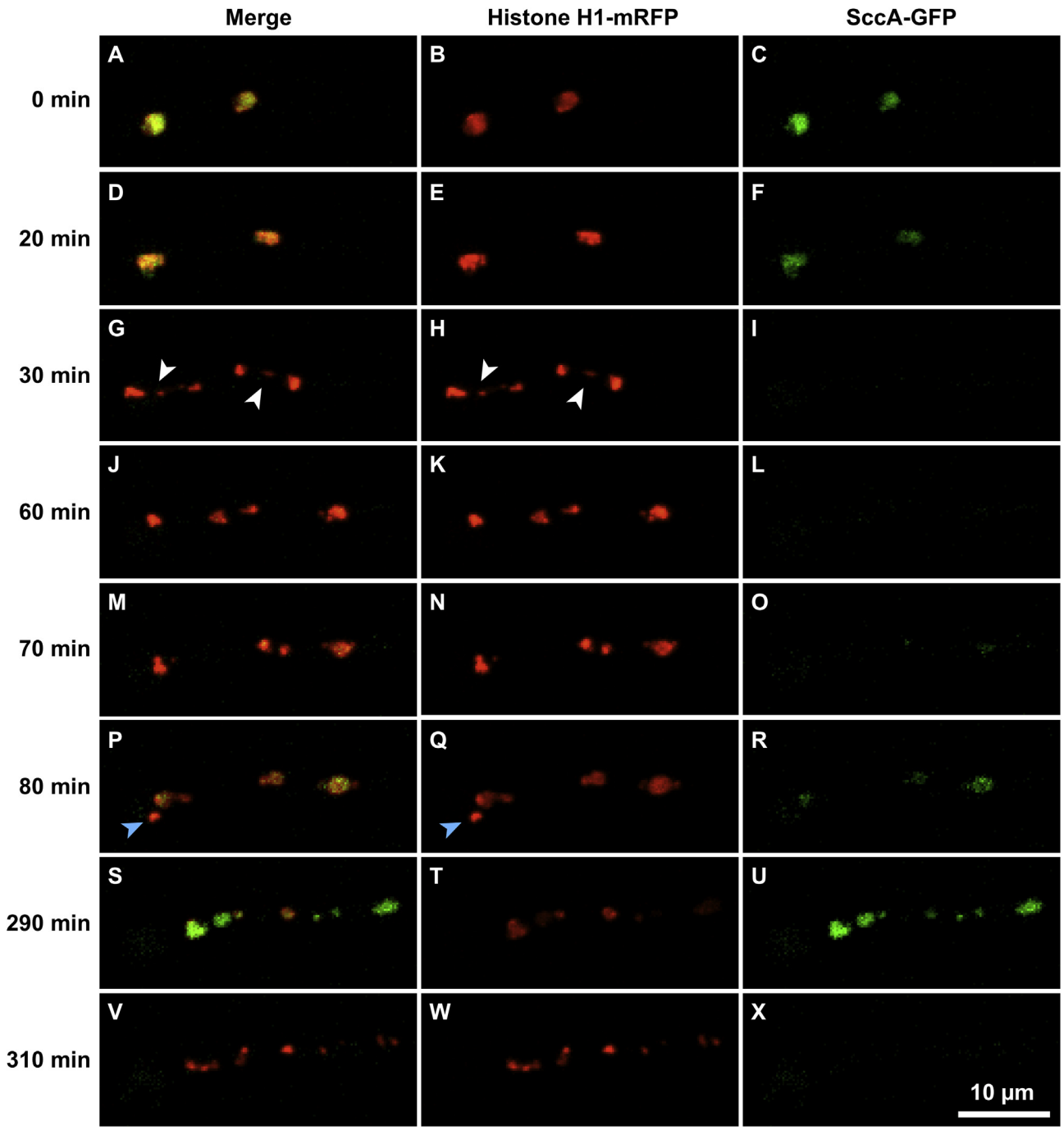

Fig. 9. SccA-GFP is removed from chromatin in db2Δ-ClbA expressing strains. Conidia from strain LO11211 (which carries *nmtA*(p)-db2Δ-*clbA*, SccA-GFP, histone H1-mRFP) were collected from 1.0 µM thiamine plates and incubated in liquid medium without thiamine at 30 °C. Images are projections from a time-lapse data set collected at 10-min intervals at 30 °C. At T = 0 min, two nuclei are in G_2 with SccA-GFP present in the nucleoplasm, but not in the nucleoli (**A–C**). Nuclei enter mitosis with SccA-GFP still present in the nucleoplasm (**D–F**). SccA-GFP leaves chromatin during mitosis (**G–I**) despite obvious nondisjunction (arrows in **G–H**). SccA-GFP remains absent from nuclei during a lengthy mitotic block (**D–R**) (60+ min) until nuclei begin to exit mitosis (**M–R**). Not all nuclei exit mitosis at the same time (blue arrow in **P–Q** indicates a nucleus that is slow in exiting). Nuclear fragments and nuclei of different sizes are apparent during interphase (**S–U**). Fragmented chromatin enters another aberrant mitosis (**V–X**), and SccA leaves chromatin once more (**X**).

model filamentous fungus *A. nidulans* as well as 31 diverse filamentous ascomycetes. Our analyses reveal that cyclins in these species fall into three distinct groups as is the case for other eukaryotes that have been studied (Ma *et al.* 2013, Cao *et al.* 2014). Our analyses also revealed that the cyclin repertoires of *Aspergilli* and the other species in our study are remarkably similar. These species include phylogenetically diverse members of the subdivision Pezizomycotina, which includes most filamentous ascomycetes. It follows that the complement of cyclins is highly conserved throughout filamentous ascomycetes. It is worth noting, however, that there may be functional specializations of cyclins, particularly non-essential cyclins, that do not change the number or phylogenetic relationships of the cyclins.

Group I cyclins

All of the species analysed in this study have three group I cyclins that fall into three distinct clades. Two clades cluster more strongly together, and the cyclins in these two clades are B-type cyclins. The cyclins in the third clade are more similar to yeast

"Cln-like" cyclins than to B-type cyclins. Importantly, each species has only a single member of each of these three clades. Group I cyclins in filamentous ascomycetes are less numerous than in the model yeasts, *S. cerevisiae, S. pombe* and *C. albicans*. In particular, *S. cerevisiae* has nine group I cyclins, none of which are essential for cell cycle progression. The multiplicity of cyclins in *S. cerevisiae* is likely the consequence of a whole genome duplication (Wolfe & Shields 1997), resulting in functional redundancy.

Group II cyclins

Most of the species we have analysed have seven group II cyclins. Four of the seven *A. nidulans* group II cyclins have been functionally characterized to some extent. As their functions may be instructive with respect to group II cyclins in other filamentous ascomycetes, we will briefly summarise the known functions of the *A. nidulans* group II cyclins.

None of the four group II cyclins in *A. nidulans* (An-Pho80, PclA, PclB, and ClgA) are essential, and all appear to play roles in development. An-Pho80 is involved in the negative regulation of phosphate acquisition enzymes and in promoting the switch from asexual to sexual development (Wu *et al.* 2004). PclA expression is cell cycle regulated and peaks during S-phase (Schier *et al.* 2001). PclA is upregulated during the late stages of sporulation (Schier *et al.* 2001, Bathe *et al.* 2010), while PclB is upregulated at both early and late stages of sporulation (Kempf *et al.* 2013). Deletion of *pclA* reduces the number of conidia (Schier *et al.* 2001), and the effects of *pclA*Δ on sporulation are additive with the effects of *pclB*Δ (Kempf *et al.* 2013). PclA has also been shown to bind and activate $NimX^{Cdk1}$ (Schier & Fischer 2002), and it is predicted to play a role in the rapid cell divisions that occur during sporulation (Schier *et al.* 2001). Finally, deletion of *clgA* reduces vegetative growth and sporulation at higher temperatures, while also delaying and repressing the development of cleistothecia (Yu *et al.* 2014).

Interestingly, three filamentous ascomycetes have gone through gene duplication events of one or two group II cyclin members. *Aspergillus carbonarius* has two PclB-like proteins. Both *P. chrysogenum* and *P. rubens* have three PclA-like proteins and three Pho80-like proteins, while *P. digitatum* has only one copy of each. We did not find evidence for duplications of group I or group III cyclins in the species analyzed.

Group III cyclins

The majority of the species we have analysed have five group III cyclins. Only one group III cyclin, PchA, has been functionally characterized in *A. nidulans.* Deletion of *pchA* is not lethal, although *pchA*Δ reduces vegetative growth and production of conidia. Deletion of *pchA* is synthetically lethal with *pclA*Δ (Bathe *et al.* 2010, Kempf *et al.* 2013).

Functional analyses of group I cyclins

Cln-like cyclin PucA

We have now found that PucA is an essential G_1/S cyclin in *A. nidulans* that is required for cells to accumulate $NimE^{Cyclin\ B}$ and enter S-phase. We have determined that PucA promotes entry into S phase by inactivating CdhA, the activator of the APC/C, during late mitosis and G_1. Although *pucA*Δ is lethal, deletion of *pucA* in a *cdhA*Δ background is viable. This result indicates that PucA is necessary and sufficient to inactivate APC/C-CdhA at the G_1/S transition. It also reveals that no other proteins, including other cyclins, can sufficiently inactivate CdhA at the G_1/S boundary to allow cell cycle progression. If there were other sufficient mechanisms for CdhA inactivation in *A. nidulans,* deletion of *pucA* would not have been lethal. This result is different from results in other organisms that have been studied, as CdhA is typically regulated by several redundant mechanisms. In both humans and *S. cerevisiae*, multiple cyclin/CDK complexes (e.g. Cln1, Cln2, Clb5, and Clb6 in *S. cerevisiae*) phosphorylate and inactivate Cdh1 at G_1/S. APC/C-Cdh1 can also be inactivated through binding of inhibitors (e.g. EMI1 in vertebrates, Acm1 in *S. cerevisiae*, and Rca1 in *Drosophila melanogaster*), but none of these inhibitors have an obvious homolog in *A. nidulans.* Thus, although Cdh1 inactivation is regulated by multiple proteins in other organisms [reviewed in Sivakumar & Gorbsky (2015)], APC/C-CdhA is essentially regulated at G_1/S in *A. nidulans* by PucA.

Although our evidence indicates that deletion of *pucA* causes a G_1 arrest, it allows continuous nuclear growth. As *pucA*Δ nuclei increased in size, we observed a concurrent loss of both nuclear DAPI fluorescence and histone H1 fluorescence. Some *pucA*Δ nuclei would eventually overcome the G_1 block and undergo mitosis, and, in those cases, the histone H1 signal would suddenly become visible as the chromosomes condensed. This indicates that the chromatin is present in interphase nuclei, but it is very diffuse. Interestingly, this diffuse chromatin phenotype has also been observed with a deletion of $nimX^{cdk1}$ (De Souza *et al.* 2013), and $NimX^{Cdk1}$ has been shown to interact with PucA (De Souza *et al.* 2014). It is also important to note that we have worked with other mutants that result in very large, stretched nuclei (e.g. the ɣ-tubulin mutant *mipA*D159), but these nuclei have very bright histone H1 fluorescence and are obviously polyploid. It is likely that deletion of *pucA* inhibits DNA replication but not nuclear growth, resulting in large nuclei with diffuse chromatin. It is also possible that this phenotype is caused by a lack of NimX activity, as PucA is a binding partner of NimX and both *pucA*Δ and $nimX^{cdk1}$Δ result in similar phenotypes.

PucA also has non-essential functions in interphase in addition to inactivating APC/C-CdhA at the G_1/S transition. In *pucA*Δ, *cdhA*Δ double mutant strains we observed nuclear abnormalities such as severe stretching and partial condensation and decondensation of chromatin in a nuclear autonomous fashion. These interesting interphase phenotypes are not due to obvious microtubule abnormalities, inhibition of polarized growth, or failure to accumulate $NimE^{Cyclin\ B}$ in the nucleus or at the SPB.

B-type cyclins ClbA and $NimE^{Cyclin\ B}$

Prior to this study, the B-type cyclin NimE was the only cyclin shown to be essential in *A. nidulans* and the only cyclin with clear cell cycle regulatory functions. The *nimE* gene was identified more than 40 years ago (Morris 1975) and found to be required for both S-phase and entry into mitosis (Morris 1975, Bergen *et al.* 1984). We have now analysed the functions of a second B-type cyclin, which we have named ClbA.

We have found that ClbA localizes to KTs from mid-G_2 until mitotic onset. *clbA* is not essential, but expression of a version of ClbA with two d-boxes deleted (db2Δ-ClbA) completely blocked colonial growth. To carry out this work, we needed to develop a more tractable repressible promoter system than the *alcA*

system that has been used extensively in *A. nidulans.* We found that the *nmtA* promoter was strongly repressible and regulatable with thiamine and this provided us with the ability to determine the phenotypes of db2Δ-ClbA expression via microscopy. We found that expressing db2Δ-ClbA resulted in mitotic catastrophe at anaphase with a high frequency of chromosomal non-disjunction as well as a mitotic arrest. Expression of db2Δ-ClbA-GFP resulted in abundant GFP signals at KTs and nuclei throughout interphase, but, interestingly, we observed that db2Δ-ClbA-GFP was still removed from KTs at mitotic entry. This indicates that ClbA is removed from kinetochores by a mechanism other than destruction. However, db2Δ-ClbA-GFP remained present in the nucleoplasm, and when anaphase occurred, db2Δ-ClbA-GFP could be seen along the spindle and at the poles of nuclei in aberrant anaphases. This was in contrast to full-length ClbA-GFP which was never seen in nuclei or at the poles during anaphase/telophase, whether overexpressed or expressed only from its native promoter. In addition, we found that expression of db2Δ-ClbA-GFP caused a lengthening of interphase. The facts that ClbA-GFP is removed from kinetochores at mitotic entry and that expression of db2Δ-ClbA-GFP causes a lengthening of interphase suggest ClbA might have a role in the G_2/M checkpoint in addition to its role mitotic progression.

Expression of dbΔ-NimE$^{Cyclin\ B}$-GFP has been shown previously to cause a mitotic block in telophase with dbΔ-NimE$^{Cyclin\ B}$-GFP remaining at the poles (De Souza *et al.* 2009, Nayak *et al.* 2010). Our use of the *nmtA* promoter to regulate expression of dbΔ-NimE$^{Cyclin\ B}$-GFP has allowed us to determine that its expression also causes a high frequency of non-disjunction. Destruction of both ClbA and NimE$^{Cyclin\ B}$ are, thus, required for chromosomal disjunction in mitosis.

We also determined that the high frequency of chromosomal nondisjunction observed in both db2Δ-ClbA-GFP and dbΔ-NimE$^{Cyclin\ B}$-GFP cells was not caused by a failure of removal of the cohesin complex. For disjunction to occur successfully, two processes must occur. The cohesin complex must be removed and catenanes (DNA intertwinings) of the daughter chromatids must be resolved by topoisomerase II. Since the cohesin complex is removed in strains expressing db2Δ-ClbA or dbΔ-NimE$^{Cyclin\ B}$, it follows that destruction of both ClbA and NimE-$^{Cyclin\ B}$ are required for DNA decatenation, presumably through regulation of topoisomerase II. Indeed, the phenotypes we observe are consistent with a failure of decatenation. Unlike the cohesin complex, catenanes cannot resist the pulling forces of microtubules [reviewed in Haarhuis *et al.* (2014)]. A failure to resolve catenanes would not block anaphase but is predicted to lead to chromosome stretching and failure of disjunction, as we have observed.

Summary of cell cycle regulation by group I cyclins in filamentous ascomycetes

Now that the three group I cyclins have been substantially characterized in *A. nidulans*, it is clear that they have distinct, non-redundant functions in cell cycle regulation. Our current findings, and previous findings from other labs, greatly clarify the functions of group I cyclins in cell cycle regulation in *A. nidulans*, and we will now summarise what we know about those functions. We anticipate, given the conservation of group I cyclins, that many of these findings will apply to other filamentous ascomycetes.

Starting our summary at the G_1/S transition, PucA activity is required to inactivate APC/C-CdhA and allow accumulation of NimE$^{Cyclin\ B}$ and consequent entry into S-phase. NimE$^{Cyclin\ B}$ is required for S-phase and for entry into mitosis. Non-degradable ClbA, but not non-degradable NimE$^{Cyclin\ B}$, causes a delay in interphase, so destruction of ClbA is important for normal progression through interphase. This fact, along with the fact that ClbA is removed from kinetochores at mitotic onset, leads us to speculate that ClbA may play an inhibitory role in the G_2-to-M checkpoint. Destruction of both ClbA and NimE$^{Cyclin\ B}$ during mitosis is required for chromosomal disjunction (likely through topoisomerase II resolution of catenanes) and removal of NimE$^{Cyclin\ B}$ from the SPB (which is normally brought about by destruction of NimE$^{Cyclin\ B}$ earlier in mitosis) is required for the M-to-G_1 transition.

ACKNOWLEDGEMENTS

Supported by Grant GM031837 from the NIH and by the Irving S. Johnson Fund of the University of Kansas Foundation. VP was supported by a graduate fellowship from the University of Kansas. We thank Dr. Mark Holder for advice concerning phylogenetic analyses. We thank Elizabeth Oakley for critical reading of the manuscript, Dr. Tania Nayak, Dr. Heather Edgerton and Dr. Yi Xiong for construction of *sccA*-GFP, and the many persons mentioned in the text for reagents that made this work possible.

APPENDIX A. SUPPLEMENTARY DATA

Supplementary data related to this article can be found at https://doi.org/10.1016/j.simyco.2018.06.002.

REFERENCES

Barlow AL, Macleod A, Noppen S, *et al.* (2010). Colocalization analysis in fluorescence micrographs: verification of a more accurate calculation of pearson's correlation coefficient. *Microscopy and Microanalysis* **16**: 710–724.

Bathe F, Kempf C, Osmani SA, *et al.* (2010). Functional characterization of a new member of the Cdk9 family in *Aspergillus nidulans*. *Eukaryotic Cell* **9**: 1901–1912.

Bergen LG, Morris NR (1983). Kinetics of the nuclear division cycle of *Aspergillus nidulans*. *Journal of Bacteriology* **156**: 155–160.

Bergen LG, Upshall A, Morris NR (1984). S-phase, G2, and nuclear division mutants of *Aspergillus nidulans*. *Journal of Bacteriology* **159**: 114–119.

Bok JW, Hoffmeister D, Maggio-Hall LA, *et al.* (2006). Genomic mining for *Aspergillus* natural products. *Chemistry & Biology* **13**: 31–37.

Campbell RE, Tour O, Palmer AE, *et al.* (2002). A monomeric red fluorescent protein. *Proceedings of the National Academy of Sciences of the United States of America* **99**: 7877–7882.

Cao L, Chen F, Yang X, *et al.* (2014). Phylogenetic analysis of CDK and cyclin proteins in premetazoan lineages. *BMC Evolutionary Biology* **14**: 10.

Costes SV, Daelemans D, Cho EH, *et al.* (2004). Automatic and quantitative measurement of protein-protein colocalization in live cells. *Biophysical Journal* **86**: 3993–4003.

Davidson G, Shen J, Huang YL, *et al.* (2009). Cell cycle control of wnt receptor activation. *Developmental Cell* **17**: 788–799.

De Souza CP, Hashmi SB, Nayak T, *et al.* (2009). Mlp1 acts as a mitotic scaffold to spatially regulate spindle assembly checkpoint proteins in *Aspergillus nidulans*. *Molecular Biology of the Cell* **20**: 2146–2159.

De Souza CP, Hashmi SB, Osmani AH, *et al.* (2013). Functional analysis of the *Aspergillus nidulans* kinome. *PLoS One* **8**: e58008.

De Souza CP, Hashmi SB, Osmani AH, *et al.* (2014). Application of a new dual localization-affinity purification tag reveals novel aspects of protein kinase biology in *Aspergillus nidulans*. *PLoS One* **9**: e90911.

Dohn Jr JWJr., Grubbs AW, Oakley CE, *et al*. (2018). New multi-marker strains and complementing genes for *Aspergillus nidulans* molecular biology. *Fungal Genetics and Biology* **111**: 1–6.

Edgerton-Morgan H, Oakley BR (2012). γ-Tubulin plays a key role in inactivating APC/C(Cdh1) at the G(1)-S boundary. *Journal of Cell Biology* **198**: 785–791.

Fernandez-Abalos JM, Fox H, Pitt C, *et al*. (1998). Plant-adapted green fluorescent protein is a versatile vital reporter for gene expression, protein localization and mitosis in the filamentous fungus, *Aspergillus nidulans*. *Molecular Microbiology* **27**: 121–130.

Fukushima H, Ogura K, Wan L, *et al*. (2013). SCF-mediated Cdh1 degradation defines a negative feedback system that coordinates cell-cycle progression. *Cell Reports* **4**: 803–816.

Haarhuis JH, Elbatsh AM, Rowland BD (2014). Cohesin and its regulation: on the logic of X-shaped chromosomes. *Developmental Cell* **31**: 7–18.

Hungerbuehler AK, Philippsen P, Gladfelter AS (2007). Limited functional redundancy and oscillation of cyclins in multinucleated *Ashbya gossypii* fungal cells. *Eukaryotic Cell* **6**: 473–486.

Hydbring P, Malumbres M, Sicinski P (2016). Non-canonical functions of cell cycle cyclins and cyclin-dependent kinases. *Nature Reviews: Molecular Cell Biology* **17**: 280–292.

Jimenez J, Ricco N, Grijota-Martinez C, *et al*. (2013). Redundancy or specificity? The role of the CDK Pho85 in cell cycle control. *International Journal of Biochemistry and Molecular Biology* **4**: 140–149.

Katoh K, Rozewicki J, Yamada KD (2017). MAFFT online service: multiple sequence alignment, interactive sequence choice and visualization. *Briefings in Bioinformatics*. https://doi.org/10.1093/bib/bbx108.

Kempf C, Bathe F, Fischer R (2013). Evidence that two Pcl-like cyclins control Cdk9 activity during cell differentiation in *Aspergillus nidulans* asexual development. *Eukaryotic Cell* **12**: 23–36.

Kocsube S, Perrone G, Magista D, *et al*. (2016). *Aspergillus* is monophyletic: Evidence from multiple gene phylogenies and extrolites profiles. *Studies in Mycology* **85**: 199–213.

Letunic I, Bork P (2016). Interactive tree of life (iTOL) v3: an online tool for the display and annotation of phylogenetic and other trees. *Nucleic Acids Research* **44**: W242–W245.

Lim S, Kaldis P (2013). Cdks, cyclins and CKIs: roles beyond cell cycle regulation. *Development* **140**: 3079–3093.

Liu D, Finley Jr RLJr. (2010). Cyclin Y is a novel conserved cyclin essential for development in Drosophila. *Genetics* **184**: 1025–1035.

Lukas C, Sorensen CS, Kramer E, *et al*. (1999). Accumulation of cyclin B1 requires E2F and cyclin-A-dependent rearrangement of the anaphase-promoting complex. *Nature* **401**: 815–818.

Ma Z, Wu Y, Jin J, *et al*. (2013). Phylogenetic analysis reveals the evolution and diversification of cyclins in eukaryotes. *Molecular Phylogenetics and Evolution* **66**: 1002–1010.

Malagon F (2013). RNase III is required for localization to the nucleoid of the 5′ pre-rRNA leader and for optimal induction of rRNA synthesis in *E. coli*. *RNA* **19**: 1200–1207.

Manders EMM, Verbeek FJ, Aten JA (1993). Measurement of colocalization of objects in dual-color confocal images. *Journal of Microscopy-Oxford* **169**: 375–382.

Martin MA, Osmani SA, Oakley BR (1997). The role of γ-tubulin in mitotic spindle formation and cell cycle progression in *Aspergillus nidulans*. *Journal of Cell Science* **110**(Pt 5): 623–633.

Martin-Castellanos C, Blanco MA, de Prada JM, *et al*. (2000). The puc1 cyclin regulates the G1 phase of the fission yeast cell cycle in response to cell size. *Molecular Biology of the Cell* **11**: 543–554.

Maundrell K (1990). nmt1 of fission yeast. A highly transcribed gene completely repressed by thiamine. *Journal of Biological Chemistry* **265**: 10857–10864.

May GS, Adams TH (1997). The importance of fungi to man. *Genome Research* **7**: 1041–1044.

Measday V, Moore L, Retnakaran R, *et al*. (1997). A family of cyclin-like proteins that interact with the Pho85 cyclin-dependent kinase. *Molecular and Cellular Biology* **17**: 1212–1223.

Meyer V, Andersen MR, Brakhage AA, *et al*. (2016). Current challenges of research on filamentous fungi in relation to human welfare and a sustainable bio-economy: a white paper. *Fungal Biology and Biotechnology* **3**: 6.

Mikolcevic P, Sigl R, Rauch V, *et al*. (2012). Cyclin-dependent kinase 16/PCTAIRE kinase 1 is activated by cyclin Y and is essential for spermatogenesis. *Molecular and Cellular Biology* **32**: 868–879.

Miller MA, Pfeiffer W, Schwartz T (2010). Creating the CIPRES science gateway for inference of large phylogenetic trees. In: *Proceedings of the Gateway Computing Environments Workshop (GCE), New Orleans, LA*: 1–8.

Morris NR (1975). Mitotic mutants of *Aspergillus nidulans*. *Genetical Research* **26**: 237–254.

Murray AW, Solomon MJ, Kirschner MW (1989). The role of cyclin synthesis and degradation in the control of maturation promoting factor activity. *Nature* **339**: 280–286.

Nalley L, Tsiboe F, Durand-Morat A, *et al*. (2016). Economic and environmental impact of rice blast pathogen (*Magnaporthe oryzae*) alleviation in the United States. *PLoS One* **11**: e0167295.

Nayak T, Edgerton-Morgan H, Horio T, *et al*. (2010). γ-tubulin regulates the anaphase-promoting complex/cyclosome during interphase. *Journal of Cell Biology* **190**: 317–330.

Nayak T, Szewczyk E, Oakley CE, *et al*. (2006). A versatile and efficient gene-targeting system for *Aspergillus nidulans*. *Genetics* **172**: 1557–1566.

O'Connell MJ, Osmani AH, Morris NR, *et al*. (1992). An extra copy of *nimE*$^{cyclin\ B}$ elevates pre-MPF levels and partially suppresses mutation of *nimT*^{cdc25} in *Aspergillus nidulans*. *EMBO Journal* **11**: 2139–2149.

Oakley CE, Edgerton-Morgan H, Oakley BR (2012). Tools for manipulation of secondary metabolism pathways: rapid promoter replacements and gene deletions in *Aspergillus nidulans*. *Methods in Molecular Biology* **944**: 143–161.

Osmani SA, Engle DB, Doonan JH, *et al*. (1988). Spindle formation and chromatin condensation in cells blocked at interphase by mutation of a negative cell cycle control gene. *Cell* **52**: 241–251.

Osmani AH, Oakley BR, Osmani SA (2006). Identification and analysis of essential *Aspergillus nidulans* genes using the heterokaryon rescue technique. *Nature Protocols* **1**: 2517–2526.

Osmani AH, van Peij N, Mischke M, *et al*. (1994). A single p34^{cdc2} protein kinase (encoded by *nimX*^{cdc2}) is required at G1 and G2 in *Aspergillus nidulans*. *Journal of Cell Science* **107**(Pt 6): 1519–1528.

Pagano L, Caira M, Candoni A, *et al*. (2006). The epidemiology of fungal infections in patients with hematologic malignancies: the SEIFEM-2004 study. *Haematologica* **91**: 1068–1075.

Schier N, Fischer R (2002). The *Aspergillus nidulans* cyclin PclA accumulates in the nucleus and interacts with the central cell cycle regulator NimX^{Cdc2}. *FEBS Letters* **523**: 143–146.

Schier N, Liese R, Fischer R (2001). A Pcl-like cyclin of *Aspergillus nidulans* is transcriptionally activated by developmental regulators and is involved in sporulation. *Molecular and Cellular Biology* **21**: 4075–4088.

Shaner NC, Campbell RE, Steinbach PA, *et al*. (2004). Improved monomeric red, orange and yellow fluorescent proteins derived from *Discosoma* sp. red fluorescent protein. *Nature Biotechnology* **22**: 1567–1572.

Sivakumar S, Gorbsky GJ (2015). Spatiotemporal regulation of the anaphase-promoting complex in mitosis. *Nature Reviews: Molecular Cell Biology* **16**: 82–94.

Sorensen CS, Lukas C, Kramer ER, *et al*. (2001). A conserved cyclin-binding domain determines functional interplay between anaphase-promoting complex-Cdh1 and cyclin A-Cdk2 during cell cycle progression. *Molecular and Cellular Biology* **21**: 3692–3703.

Stamatakis A (2014). RAxML version 8: a tool for phylogenetic analysis and post-analysis of large phylogenies. *Bioinformatics* **30**: 1312–1313.

Subach OM, Cranfill PJ, Davidson MW, *et al*. (2011). An enhanced monomeric blue fluorescent protein with the high chemical stability of the chromophore. *PLoS One* **6**: e28674.

Szewczyk E, Nayak T, Oakley CE, *et al*. (2006). Fusion PCR and gene targeting in *Aspergillus nidulans*. *Nature Protocols* **1**: 3111–3120.

Tamm T (2012). A thiamine-regulatable epitope-tagged protein expression system in fission yeast. *Methods in Molecular Biology* **824**: 417–432.

Toews MW, Warmbold J, Konzack S, *et al*. (2004). Establishment of mRFP1 as a fluorescent marker in *Aspergillus nidulans* and construction of expression vectors for high-throughput protein tagging using recombination in vitro (GATEWAY). *Current Genetics* **45**: 383–389.

Vishniac W, Santer M (1957). The thiobacilli. *Bacteriological Reviews* **21**: 195–213.

de Vries RP, Riley R, Wiebenga A, *et al*. (2017). Comparative genomics reveals high biological diversity and specific adaptations in the industrially and medically important fungal genus *Aspergillus*. *Genome Biology* **18**: 28.

Wang H, Xu Z, Gao L, *et al*. (2009). A fungal phylogeny based on 82 complete genomes using the composition vector method. *BMC Evolutionary Biology* **9**: 195.

Wolfe KH, Shields DC (1997). Molecular evidence for an ancient duplication of the entire yeast genome. *Nature* **387**: 708–713.

Wong RW (2010). An update on cohesin function as a 'molecular glue' on chromosomes and spindles. *Cell Cycle* **9**: 1754–1758.

Wu D, Dou X, Hashmi SB, *et al*. (2004). The Pho80-like cyclin of *Aspergillus nidulans* regulates development independently of its role in phosphate acquisition. *Journal of Biological Chemistry* **279**: 37693–37703.

Xiong Y, Oakley BR (2009). In vivo analysis of the functions of γ-tubulin-complex proteins. *Journal of Cell Science* **122**: 4218–4227.

Yang L, Ukil L, Osmani A, *et al*. (2004). Rapid production of gene replacement constructs and generation of a green fluorescent protein-tagged centromeric marker in *Aspergillus nidulans*. *Eukaryotic Cell* **3**: 1359–1362.

Yu Z, Cai M, Hu W, *et al*. (2014). A cyclin-like protein, ClgA, regulates development in *Aspergillus nidulans*. *Research in Microbiology* **165**: 462–467.

Yu JH, Hamari Z, Han KH, *et al*. (2004). Double-joint PCR: a PCR-based molecular tool for gene manipulations in filamentous fungi. *Fungal Genetics and Biology* **41**: 973–981.

Zarrin M, Leeder AC, Turner G (2005). A rapid method for promoter exchange in *Aspergillus nidulans* using recombinant PCR. *Fungal Genetics and Biology* **42**: 1–8.

Zi Z, Zhang Z, Li Q, *et al*. (2015). CCNYL1, but not CCNY, cooperates with CDK16 to regulate spermatogenesis in mouse. *PLoS Genetics* **11**: e1005485.